Environmental transformations of Manganese and Manganese oxide nanoparticles

ANNIE LUNDBERG

Abstract

Engineered nanoparticles (NPs) are produced in increased quantities. Due to this increase, it is vital to understand the full lifecycle and fate of these NPs to prevent any possible environmental stress. As a result of their size, NPs may interact differently with their environment compared to bulk materials with the same composition, this both gives NPs their usage as well as risks. The risks often include unwanted interaction with biological systems which may lead to generation of toxicity. This study focused on environmental transformations of manganese and manganese oxide (Mn_3O_4) NPs. Applications these nanoparticles are often in battery technology and catalysis. A solution intended to mimic the composition of freshwater was used as the environmental media to study these transformations. Exposure of NPs was performed both with and without added natural organic matter (NOM). Several experiments were preformed such as Atomic absorption spectroscopy (AAS) for dissolution of the NPs, Nanoparticle Tracking Analysis (NTA) for particle size, and Attenuated total reflection Fourier transform infrared spectroscopy (ATR-FTIR) for adsorption studies. The production of reactive oxygen species (ROS) was also investigated, and simulations of metal speciation using Visual MINTEQ were also performed.

The results from NTA and AAS (for Mn_3O_4) were not very reliable due to inconsistencies in the results which were probably caused by problems with preparation. However, for both, the results point towards that the dissolution rates of the particles are slightly slowed down when NOM is added. From ATR-FTIR and the simulations it was confirmed that NOM, carbonate, and sulfur will adsorb onto both particles, possibly in multiple layers. As for increased ROS development, no evidence of such an increase was found. However, the method used does not test for increased hydrogen peroxide development so this would in interesting test as well. Other studies which also would contribute to a more nuanced picture of this system is studies regarding zeta potential and studies which further investigates the type of adsorption mechanism which occurs at the particles surface.

Sammanfattning

Industriella nanopartiklar används i allt större utsträckning. Därför är det av stor vikt att undersöka hela livscykeln som dessa produkter går igenom for att säkerhetsställa att de inte utgör någon fara för miljön och ekosystemen som de kan komma att hamna i. Som ett resultat av deras storlek interagerar nanopartiklar annorlunda med sin omgivning om man jämför med bulkmaterial av samma sammansättning, detta nanopartiklar både sina unika fördelar och risker. Riskerna innefattar ofta oönskade interaktioner med biologiska kretslopp som kan resultera i toxicitet. I den här rapporten läggs fokus på just denna typ av kemiska omvandlingar som nanopartiklar av mangan och manganoxid kan tänkas genomgå i det naturliga kretsloppet. Applikationer man ofta ser dessa partiklar i är batteriteknologi och katalys. De medium som används för att studera omvandlingarna är en lösning som efterliknar ytvatten från en klar sjö. Exponeringar gjordes både med denna lösning så som den är och med tillsatt naturligt organiskt material, NOM.En rad olika experiment gjordes så som analyser med AAS för att undersöka partiklarnas upplösning, NTA för partikelstorlekar och ATR-FTIR som undersökte adsorption på partiklarna. Även en studie med en DCFH metod där ökat ROS aktivitet undersöktes och en rad med SHM simuleringar gjorda i Visual MINTEQ utfördes.

Resultaten från NTA och AAS analysen visade sig inte vara särskilt tillförlitliga på grund av tvetydliga resultat som troligen orsakats av problem med provpreparationen. Men resultaten från båda dessa pekar mot att upplösningshastigheten blir något hämmad då man tillsätter naturligt organiskt material, för båda partiklarna. Från ART-FTIR och simuleringarna kunde de säkerhetsställas att adsorption av NOM, karbonat och svavel sker på båda partiklarna, möjligen i fler än ett lager. När det kommer till ROS studien kunde inga bevis på ökad ROS aktivitet hittas med den använda metoden. Dock så kunde inte ökat väteperoxid aktivitet mätas med den metod som användes så detta hade varit av intresse att testa i framtiden. Andra studier som också skulle vara hjälpsamma för att ge en mer nyanserad bild av detta system är en studie om partiklarnas zeta potential och mer undersökningar om vilken typ av adsorptions mekanism som sker vid partiklarnas yta.

List of Abbreviations

AAS	Atomic absorption spectroscopy
Ag NPs	Silver nanoparticles
DCFA-DA	Dichlorodihydrofluorescein diacetate
DCFH	20 7- dichlorodihydrofluorescein
DLS	Dynamic light scattering
ETAAS	Electrothermal atomic absorption spectrometry
FA	Fulvic acid
FW	Freshwater
GF-AAS	Graphite Furnace Atomic absorption spectroscopy
HCL	Hollow cathode lamp
HA	Humic acid
NMs	Nanomaterials
NOM	Natural organic matter
NPs	Nanoparticles
ROS	Reactive oxygen species
SCM	Surface complexation model
SHM	Stockholm humic model
UV-vis	Ultraviolet-visible spectroscopy
ZP	Zeta potential

Table of Contents

1. Introduction

A nanomaterial (NM) is defined to have at least one dimension in the range of 1-100 nm. NMs and NPs occur naturally and abundantly because of both anthropogenic and natural processes [1].

The rapid development of nanotechnology has resulted in new complex materials and applications using nano-sized and nanostructured materials [2] [3]. Due to this growth, it is important to evaluate and understand the physical and chemical properties of engineered nanoparticles (NPs) since their presence are likely to increase in the biosphere [4]. This understanding includes environmental implications, which will ensure compliance with environmental guidelines. Studies that examine the fate, toxicity and transformation of NPs are therefore of importance for sustainable production and knowledge of the lifecycle of NPs [5]. Investigations of this nature often aim to study the surface interactions of the particles in contact with environmental-relevant media. This often corresponds to adding the NPs to a solution which contains constituents (salts, organic matter, etc.) that are also present in the environment, and then examining the adsorption and other interactions of these with the NP surface [6] [7] [8].

Both manufactured and natural NPs has a high percentage of surface atoms due to their small size, and this may result in different properties and reactivities compared to bulk materials with the same composition [9] [10]. Gold nanoparticles are for example catalytic, opposed to larger size gold particles, which are typically inert [11]. NPs also inherently have a very high free energy due to the high surface curvature. Thermodynamic driving forces will counteract this to minimize the energy. This can, depending on surroundings, result in numerous physical and chemical transformations such as agglomeration of particles, dissolution, and ligand adsorption [12].

Environmental and safety concerns regarding the use of engineered NMs have been raised due to the in some cases different properties compared with bulk materials, resulting in increased toxicity compared with larger sized particles [4] [13]. It is hence important to understand the difference mechanism of NP that appears due to their size. These transformations can be sensitive to factors such as pH, ionic strength, and composition. The surface of a NP might undergo significant changes regarding composition and various properties over time depending on the surrounding conditions [14] [6] [15]. Investigating this requires understanding of potential and common exposure environments and the toxicological implication of the exposure, both acute and chronic. However, due to their extremely small size and reactivity, NMs are often very dynamic in environmental systems and therefor difficult to study since they may undergo processes like adsorption, dissolution, changes in chemical composition and so on. Also, any transformations which the NMs undergo will affect their fate, toxicity, and transport properties. An example of this is silver NPs which may be oxidized and sulfurized in some environments. The sulfidation changes the NPs aggregation state, surface chemistry, and the release of toxic Ag^+ ions [16]. This in turn will affect the NPs' toxicity and persistency in the environment. In a similar

manner, natural organic matter (NOM) can create a nanoscale coating on metallic NPs which in turn dramatically can change their toxicity, agglomeration, and deposition [17] [18] [19].

It is very challenging to determine the risks that are associated with releasing NPs into the environment since environmental systems consist of multiple processes which are dynamic and stochastic. Several processes can affect the transformations of NPs in the environment, such as dissolution, agglomeration, adsorption, and redox reactions. For some NPs these may decrease the toxicity, while for others they may enhance it. For example, silver NPs are likely to become sulfidized in nature. Due to the sulfidation, properties such as agglomeration state, surface chemistry as well as the NPs ability to dissolve into toxic Ag^+ ions, which in turn affects their toxicity and persistence in the system [16]. Also, another example of this is the adsorption of humic substances such as NOM. The adsorption forms a nanoscale film on the NPs which affects their surface properties, this in tur affects toxicity, persistence, and agglomeration of the NPs. However there still exists uncertainty about how such transformation affect the lifecycle and behavior of many NMs [4].

1.1 Ethical aspects

Furthermore, the goals of this project also a line well with some of FN;s global goals regarding sustainability and the environment. Goal 9 and 15, in particular, matches well with the study. Goal 15 aims protect the biodiversity and ecosystems [20]. This is supported by the project since it examines the possible dangers and effects of increased amounts of NP:s in nature to ensure that this will not cause an environmental threat. Part of goal 9 is to ensure a sustainable and innovative industry [21]. In this project this goal is represented by the project's goal of making it easier to include nanotechnology in the technological development to facilitate an innovative but safe development. Today it can be quite challenging to include NM:s in products and development since it is hard to ensure the safety, including environmental safety. However, if the risks associated to NM:s are determined it will also be easier to include them in more development which is likely to lead to more new applications and products.

2. Motivation and Aim of study

This study aims to investigate the various environmental transformation of manganese (Mn) and manganese oxide (Mn_3O_4) NPs. This is important to investigate since manganese oxides have multiple interesting uses such as magnetic materials, ion-sieves, catalysts, batteries, and water treatment [22] [23] [24] [25]. Furthermore, manganese- based NPs can be used as contrast agents in different imaging techniques such as magnetic resonance imaging [26].

When investigating the toxicity of NPs one aspect of interest is if the NPs facilitate generation of ROS. ROS is commonly defined as oxygen related or oxygen centered ions, radicals, or molecules [27]. Excessive generation of ROS is likely to pose an environmental hazard since it may cause oxidative stress. Oxidative stress refers to a state in which antioxidants cannot neutralize the ROS fast enough compared to the production of them, causing an imbalance. This may lead to severe damage to cellular components such as proteins, lipids, metabolites, and nucleic acids [28]. The ROS-related toxicity of certain NPs is

influenced by the ability of NP to generate ROS. The NPs capacity to generate ROS has become an important subject when investigating nanotoxicology due to both NPs being more commonly used in everyday products and the significant role that generation of ROS has on the toxicity of NPs [29] [30] [31]. An increase in oxidative stress has been found for Mn- and Mn_3O_4 NPs, although the oxide form of manganese showed a lot less toxicity [32] [33]. Due to this, there is a need for studies who focuses on environmental transformations which may influence the toxicity of manganese and manganese oxide NPs.

In this study, transformation caused by exposure in two different media will be investigated. These transformations include dissolution and agglomeration behavior, as well as adsorption and ROS generation.

The solutions aim to mimic FW and FW containing NOM. The analytic equipment used to study these transformations were AAS, ATR-FTIR, NTA, and ROS detection. Additionally, MINTEQ was used to simulate metal complexation to NOM and inorganic components of NOM. The addition of NOM to suspensions containing NP has shown to impact several environmental transformations of the particles, ROS generation among them, and is therefore important to consider [34].

The project is also a part of the interdisciplinary research programme Mistra Environmental Nanosafety. This programme aims to ensure a safe a development of nanotechnology. To do this it focuses on developing sufficient research, knowledge, and asses the risks associated with NMs and the impact they may have on both health and the environment. The goal is to access these risks and suggest safe innovative policies when it comes to the use of NMs. This project fits in well with the programme since transformations of NPs caused by the environment is an important part of assessing possible risks of NMs [35].

3. Background

3.1 Nanostructured manganese and manganese oxide NPs

3.1.1 Characterization pre-study

This general pre-study is meant to give insight to the original properties of the NPs used in this study. However, the pre-study was not performed by the author but still offer important knowledge about the Mn and Mn_3O_4 NPs used in the current study.

3.1.1.1 Methods and methodology

3.1.1.1.1 XRD

X-ray diffraction, XRD, was used to study the surface oxide/oxides on particles. In this case dry powders were studied by conduction several runs and then averaging the spectrums in order to minimize noise.

3.1.1.1.2 SEM

To study the surface morphology of the dry powders scanning electron microscopy, SEM, was used. This was done by adding powder to a carbon tape and attaching this to the sample holder.

3.1.1.1.3 TEM

When investigating the primary size and shape of the NPs transmission electron microscopy, TEM, was used. The ethanol solution used for TEM had a concentration of 1 g/L of particles and was sonicated for 10 min each twice while being vortexed in between.

3.1.1.1.4 ZETASIZER

The zetasizer is an instrument which can measure the zeta potential. The zeta potential refers to the potential existing in between the stationary and the diffuse layer, at the slipping plane. When a particle is put into an ionic solution it will form a surrounding layer of ions of opposite charge. These ions are stationary and therefor this layer is often referred to as the stationary or stern layer. When looking beyond the stationary layer the diffuse layer is found. The diffuse layer mostly consists of ions which are charged oppositely to the stationary layer to counteract the charge.

If the zeta potential is high the particles will have more difficulties to agglomerate due to electrostatic repulsion. Therefore, zeta potential can be useful to determine the stability of a dispersion containing the particles. Also, the zeta potential can give some indication of the surface charge is sufficient knowledge of the solution charge exists. [36] The measurement works by applying an electrical field which will induce movement of the particles. This movement is then what is measured and calculated into zeta potential by the Zetasizer. The samples for these were made from adding NP in powder form to a solution with 10 mM NaCl. Since the added particles were quite instable in solution the values mostly apply to the more stable particles.

3.1.1.2 Results

For the Mn and Mn_3O_4 NPs used in this study, surface characterization using X-ray diffraction, XRD, was preformed beforehand. [32] [37] This showed that the surface of the Mn NPs was made up of a mixed oxide containing MnO, Mn_2O_3, MnO_2 and that the surface of the Mn_2O_3 NPs was made up of both MnO and Mn_2O_3 [38]. Both particles had a negative surface charge, as seen in table 1.

Table 1. A summary of the manganese and oxide NPs characteristics.

Particle type	Zeta Potential [mV]	Shape and size of particles [nm]	Surface oxide composition
Mn	-30±7	Spherical: 15-50 Clusters: 100-200	MnO, Mn_2O_3, MnO_2
Mn₂O₃	-31±15	Cubic: 20-180 Rods (μm): $8 * 10^{-3}, 0.4 * 10^{-3}$	Mn_3O_4, MnO

When investigated in SEM the Mn NPs appear to have a large size distribution. For Mn_3O_4 fibers of 5 μm was found as well as agglomerates around 100 nm. When measuring in TEM the images showed spherical particles which were 15-50 nm as well as clusters around 100-200 nm for the Mn NPs. The Mn_3O_4 NPs, on the other hand, showed cubic particles which were around 20-180 nm as well as rods which were 8 x 0.4 μm, as seen in table 1. Figure 1 and 2 shows TEM images.
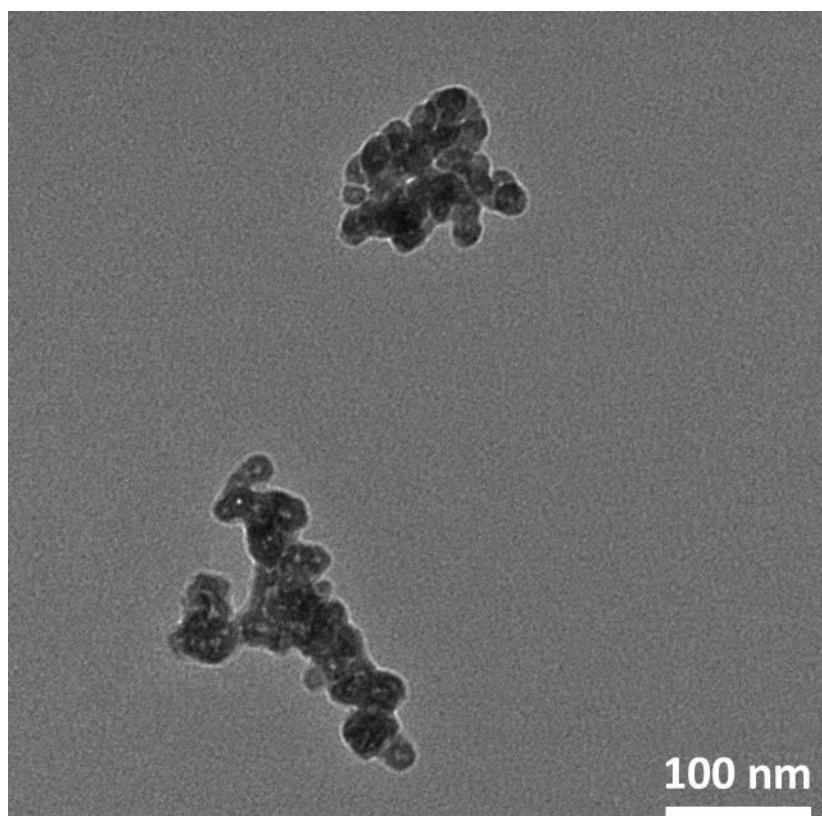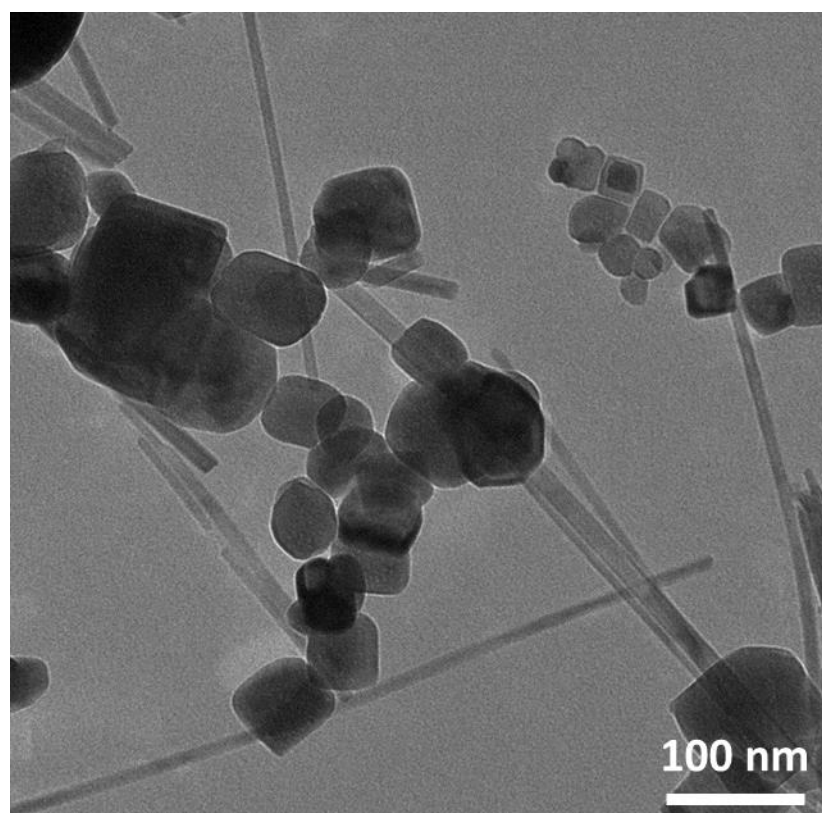
Figure 1. TEM image of Mn NPs.

Figure 2. TEM image of Mn$_3$O$_4$ NPs.

3.2 Natural organic matter

Natural organic matter (NOM) is an essential component in many environmental processes. NOM is known to play a key role in processes such as metal speciation, acid buffering, and mineral weathering in the terrestrial environment [39] [40]. The high concentration of functional groups containing elements such as sulfur, oxygen, and nitrogen in NOM is part of the reason to why NOM is such a reactive and dynamic component in natural systems. Therefor NOM is very important to consider when performing environmental investigations of NPs.

Oxygen is particularly important for due to its shear abundance, and can be found in carboxylic, alcoholic, carbonyl, and phenolic groups as well as in ethers and ester linkages in NOM. Phenolic and carboxylic groups may act as both as binding ligands for metals and a source of acid, while most of the other functional groups only act as binding ligands for metals. Carboxyl groups are more acidic then phenolic and are also the most prominent form of oxygen in NOM. Carboxylic groups are a key component in NOM in many ways as a key component in fulvic and humic acids, as they contribute the most to NOM characteristics such as acidity, charge and metal binding compared to the other functional groups [40].

Even if there is a lot of information and knowledge about the different parts and functional groups which make up NOM, their role in environmental processes is still very complicated to determine. One large reason for this is that the behavior of a functional group in NOM is highly dependent on the structural environment of the macromolecule. For example, the positions of certain atoms and how the functional groups are connected play an important role [41]. For NOM, this knowledge is poor concerning its functional groups, especially for the key carboxyl groups. One example of this is that the metal complexion strength as well as the acidity of carboxyl acids varies dependent on the coordination of the carboxyl [42] [43] [44]. Molecular configuration may also affect the metal affinity of NOM since it affects which functional groups other than carboxyl groups may participate in metal binding. Generally, metal binding reactions are predictable for a lot of small molecules, for example organic acids. However, metal binding behavior is harder to predict for more complicated and larger macromolecules [45] [46].

3.3 Surface transformations of NPs

Knowledge of dynamics at the surface is, as previously mentioned, an essential part of predicting the transformations, persistence, and fate of NPs [47]. In many cases it is difficult to capture the numerous surface processes taking place on the NP in different media, even if there is thorough categorization of NPs [4]. The aquatic media in the biosphere can be very complicated in terms of formulation. They often include, but are not limited to, proteins, NOMs, lipids, carbonates, and amino acids in various combinations and concentrations [14]. When exposed to such media, NPs can undergo transformations related to both surface and bulk of the NP depending on the surroundings. Figure 3 shows common transformations which may occur when NPs are exposed to different media [14].
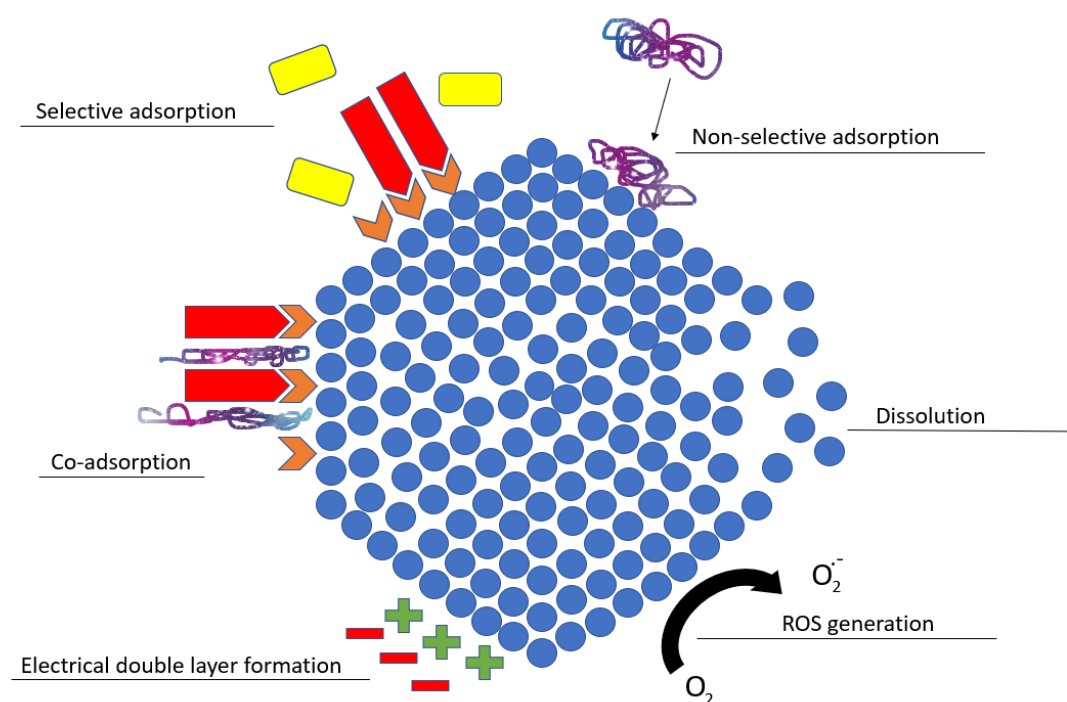
Figure 3. Schematic figure displaying different physicochemical transformations of NPs.

These transformations affect the surface composition of the NPs. Therefore, two different NPs might exhibit different surface compositions even if the medium is the same, and the same is also true for same NPs which are exposed to different media [47] [48].

3.3.1 Chemical and electrochemical transformations

Coupled processes such as oxidation and reduction, which include an exchange of electrons, are common in both aquatic and terrestrial environments [4]. These processes can affect the fate metallic NPs. NPs may contain elements which can undergo both oxidation and reduction in different natural environments. For some NPs oxidation may cause the formation of a relatively stable oxide on the surface of the NPs which in turn passivates it and reduces further oxidation, for example aluminum NPs [49]. For other more reactive metals, this protective layer will not form properly and therefore not provide sufficient protection from oxidation. These metals can therefore be oxidized and dissolve in conditions where more stable metals would not [50] [51].

Generally, oxidation processes predominantly occur in environments such as aerated soils and natural water, while reduction is the predominant process in ground water and carbon rich sediments, where there may be oxygen depletion. There are also some more dynamic areas such as tidal zones where NPs may shift and cycle between different redox states [4].

Transformations such as sulfidation and dissolution play an important role for NPs' persistence, surface properties, and toxicity [4] [52]. For metals that are soft Lewis acids, such as Zn, Cu and Ag, this is very important since they tend to form metal oxides which are partly soluble and the also have a high affinity for both organic and inorganic sulfide ligands. The toxicity of some class B metals, such as Zn, is directly linked to dissolution since the toxic

response is mostly due to toxic cations [16]. Class B metal are defined as metals which form soft acids [53]. If complete dissolution is reached some predictions regarding the toxicity may more easily be made. It is therefore important to assess the dissolution and/or sulfidation rate and behavior of NPs environmental conditions and particle properties, as this is essential to assess the toxicity of the NPs [4] [54] [55].

3.3.2 Physical transformations

Agglomeration is the process in which two or more particles forms bigger clusters with one another, called an agglomerate. These agglomerates are not bound very strongly and may separate if the properties of the solution changes. If the particles are very tightly bound, this is often referred to as aggregation. Agglomeration can occur in two different ways, one is homoagglomeration, meaning agglomeration between the same NPs, and heteroagglomeration is agglomeration between the NPs and other particles in the surrounding environment (for example iron oxide particles) [4]. It is a transformation which reduces the high surface to bulk atom ratio in NPs. Due to the increasing size of the agglomerate the reactivity, sedimentation behavior, and toxicity is affected. This transformation can over time be hard to avoid unless the NPs have engineered coatings, or something similar, which reduces the formation of agglomerates.

The number concentration of particles will, as previously implied, decrease when agglomeration occurs in a suspension, as well as raise the average particle size [56]. Therefore, a rapid agglomeration can decrease mobility of particles in the solution. If for example heteroagglomeration occurs between NPs and much larger particles, clay for example, this might change the properties of the NPs significantly if the agglomerate more closely resembles a clay particle in terms of mobility [57].

Apart from mobility, the reactivity of the NPs is also likely to be affected by agglomeration. The reason for this is that the available surface area is decreased by agglomeration. Surface atoms are much more reactive than those in the bulk, so when agglomeration occurs and the surface area decreases, the reactivity of the NPs is also likely to decrease. However, the magnitude of the decrease will depend on numerous factors such as size distribution and fractal dimension of the agglomerate [58].

Agglomeration can decrease toxicity if the reaction which results in the toxic response is related to available surface area. Both dissolution and ROS generation are examples of such transformations. It is also possible that agglomeration may increase the persistence of the NPs if it decreases the dissolution rate in comparison to the fully dispersed NPs [4].

3.3.3 Adsorption

The surface composition is highly dependent on the contents of the surrounding medium. Adsorption of constituents in FW, for example NOM, to the NPs changes their surface composition and can therefore impact properties such as reactivity, dissolution, and agglomeration. The surface composition is determined by the adsorption affinity of the ligands in the solution which interact with the particles. For example, adsorption of carbonate can result in changes to the surface charge, which in turn will alter the NPs solution phase behavior [14] [47]. The ligands with the highest affinity to the NPs will adsorb

the strongest. The adsorbed layer which is formed by these adsorbed ligands is often called "corona" [59]. In a single component medium the corona can be assumed to be quite uniform in terms of composition, but this is often not the case with more complex media. Competitive adsorption processes between the different ligands are common for these systems. Broad adsorption bands are a sign of multiple adsorbed species (*e.g.* observed with ATR-FTIR) [14]. The final surface composition of more complex systems is determined by the relative affinities of the different components towards the NPs surface [60]. However, the surface composition of the NPs can undergo changes over time depending on the affinity of the surface ligands. Ligands with low affinity can be displaced by those with higher while ligands with similar affinity for the NPs surface might co-adsorb to it. During co-adsorption, the components which are already adsorbed to the surface can rearrange to allow another species to adsorb [61] [62].

3.3.3.1 NOM adsorption

NOM must be considered when investigating environmental media adsorption on NPs. Several studies have shown that the presence of NOM can affect the aggregation behavior of NPs, showing that NOM may change the surface properties of NPs [63] [64] [65]. The presence of NOM has been proven to decrease the aggregation, but also to decrease the toxicity and uptake of some soil organisms used as test species [66].

There have been investigations on the adsorption of NOM onto manganese oxide (MnO_2). [67] [68]This knowledge is valuable since it affects fate and transportation mechanisms of both inorganic and organic pollutants in for example aquatic systems. Due to its high redox potential ($E_H^0 = 1.23\ V$), MnO_2 is often very active in redox reactions. For MnO_2 these reactions have been quite widely studied and two main steps have been established for these redox processes: complex formation at the surface and electron transfer [69].

Birnessite (δ-MnO_2), a common type of manganese oxide, is negatively charged within the pH range found in most natural waters [67]. NOM is also negatively charged in this pH range and can still be adsorbed onto birnessite despite the fact that NOM adsorption onto metal oxides is most often controlled by electrostatic attraction [70]. The NOM will compete with various inorganic/organic compounds for reaction sites at the surface of the NP, therefor the adsorption of NOM onto NPs can decrease the oxidation rates of contaminants. Since NOM adsorption alters the metal oxides surface properties it also affects the redox processes at the surface. Mobility and oxidation of pollutants, as well as mineral dissolution, might thus be highly affected by the presence of NOM in aquatic systems [69].

Other than decreasing oxidation rates of pollutants, adsorbed NOM can also be oxidized by manganese oxide. This can occur simultaneously with the oxidation of contaminants and increase the reactivity of NOM, creating a complex environment where undesirable transformation products might form. For example, studies have shown that the presence MnO_2 can facilitate methyl iodide formation, which can be potentially hazardous for the ozone layer [69].

Furthermore, it has been shown that cationic species such as Ca^{2+} and Mg^{2+} will increase the adsorption capacity of NOM to manganese oxide, this is possible since these reverse the

surface charge of the manganese oxide and therefore also increase the NOM adsorption [69].

3.4 Analysis techniques

3.4.1 AAS

Graphite furnace atomic absorption spectrometry (GF-AAS) was used to determine the concentration of released ionic Mn species, after exposure and centrifugation to remove the undissolved NPs.

In GF-AAS the sample is added to the analyzer in very precise microliter volumes. After this, the sample is vaporized and the element that is measured for is atomized. The atomized metal absorbs electromagnetic radiation that has a specific wavelength, which in turn provides a signal that is proportional to the concentration metal in the samples.

Since atoms are required to be in a gaseous state, the instrument needs to provide enough heat to achieve this. This is done using an atomizer, while there exist two main types of these, we will only focus on one of these in this study due to the low concentration of the samples, electrothermal AAS (ETAAS). Thereafter, the concentration of this element can be determined by analyzing the absorption of the atomized atoms as they are subjected to a light source with a characteristic wavelength. This light source is most commonly a hollow cathode lamp that contains the element that is of interest and the detector is typically photomultiplier tube. A monochromator is used to separate the measured element´s spectral response [71].

3.4.2 NTA

In NTA, the light scattered light from the NP movement (Brownian motion) and is to obtain the particle size distribution of particles in a liquid suspension. This is executed using a laser beam which passes through a prism-edged glass inside the sample chamber. Both the refractive index and the angle of incidence of the glass flat are tailored so that when the beam will refract when it reaches the glass and the solution. This will result in a compressed beam which has higher power density. Particles in solution which cross this beam and scatter the light can be visualized with ease due to the long working distance of the objective. The magnification ability is up to 20 times and this lens is usually attached to a typical optical microscope. A camera gear is mounted is onto this microscope (metal-oxide-semiconductor (CMOS) camera). These devices can obtain approximately 30 frames per second and capture a video file of the light scattered by the particles. In real size this video is of an area which is typically ca 100x80x10 μm. Figure 4 schematically displays a common setup for an NTA aperture.
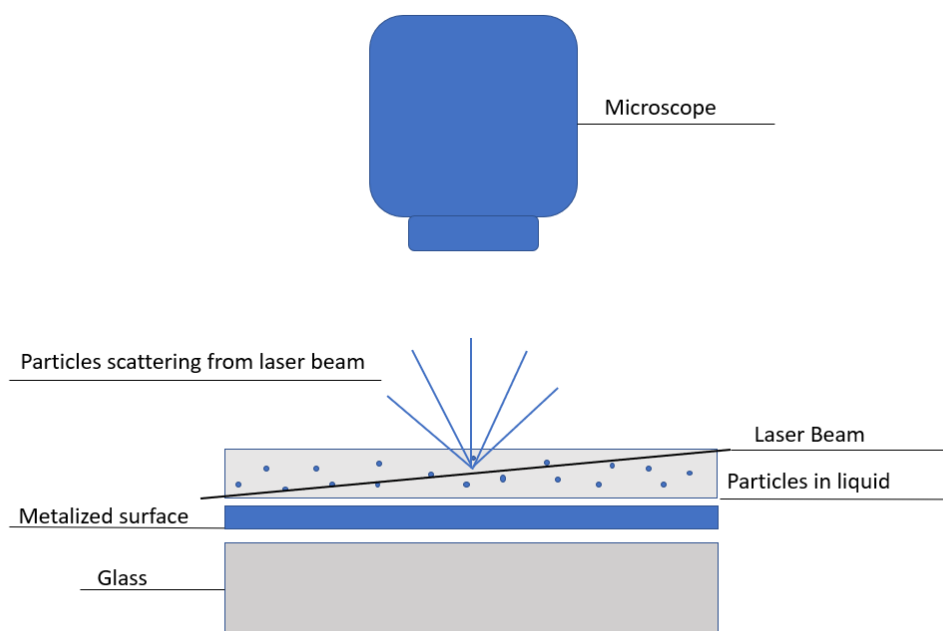
Figure 4 Schematic drawing of the NTA setup.

The NTA software can identify the particles and determine the average distances they move in x and y directions from the recorded video file. From this the diffusion constant, D_t, can be determined and then the sphere-equivalent hydrodynamic diameter(d) can be calculated by using the Stokes-Einstein formula or equation 1.

$$D_t = \frac{TK_B}{3\pi\eta d}$$
(1)

Here K_B is Boltzmann´s constant, T is the temperature and ŋ is the viscosity of the solvent [73]. One large advantage of NTA compared to other techniques is that it is not as biased towards agglomerates and larger particles when compared to some other common methods such as DLS [74].

3.4.3 ATR-IR

Attenuated total reflection, ATR, is a method based on infrared spectroscopy to enable samples in both liquid and solid states to be directly examined without the need for further preparation [75]. The technique is possible since it utilizes the total internal reflection at an interface, which results in an evanescent wave. An evanescent wave consists of an electromagnetic field whose energy is spatially concentrated near the interface. This is achieved by letting a beam of infrared light pass through the ATR crystal in a way which allows it to reflect at the very least once off the internal surface that is in contact with the sample. From this reflection an evanescent wave is created which extends into the sample if the refractive index is lower in the samples compared with the crystal and the angle of incidence is lower than the critical angle. The critical angle is defined as the angle of incidence in which a refraction of 90 degree is obtained. Typically, the depth of penetration is somewhere between 0.5-2 µm [47]. The exact penetration depth can be determined by knowing the angle of incidence, the specific refractive indices of both the ATR-crystal and

the medium, as well as the wavelength of light. When the beam exits the ATR crystal it is collected by the detector. In this case the ATR crystal is a diamond. However, the signal will decrease in the area where the diamond absorbs light, this will in turn increase the noise in this spectral region (1900-2600 cm^{-1}) [76] [75].

One advantage of this method is that that it has a limited penetration depth into the sample. This in turn avoids strong attenuation of the IR signal in aqueous solutions or other media with high absorption.

A thin and hydrated film is often placed on top of the ATR crystal when studying NPs using ATR-FTIR. When this film is exposed to different media, which for example contains NOM or inorganic salts, significant changes to the spectra can be observed. After subtraction of the signal from the aqueous solution the remaining spectra shows absorption bands originating from the vibrations of the new surface species. From such studies the diverse surface compositions of NPs depending on the surroundings can be studied [14] [75].

3.4.4 ROS

This report will focus on the 2,7- dichlorodihydrofluorescein (DCFH) analysis for detection of ROS, which is one of the most common methods. One reason for its popularity is probably because it can be oxidized by many functional groups involved with ROS without any notable preference [77]. When performing an acellular measurement with DCFH it is common to procced from the more stable compound DCFH$_2$-DA and then add a strong alkaline solution, such as NaOH, to cause deacetylation [78]. This will cause oxidation of DCFH$_2$-DA to DCF in with two oxidation processes, both using single electrons. To begin with, through electron loss of the DCFH$_2$-DA, the intermediate DCFH is formed. After this the DCFH ones again loses an electron and forms DCF. DCF is then able to form DCF* by photoexcitation during measurement [79].

DCHF has been questioned somewhat as a flourescent reactant, due to the sensitivity (self-oxidation of DCFH) regarding both light and oxygen [80]. Moreover, a uniform approach to handling DCFH has been lacking leading to a lot of different handling which may explain differing results using it. As an example, some evaluation studies found that by using different sonication protocols will impact the results [81] [82]. Due to these problems, it has been debated whenever DCFH reliable enough to be used to measure ROS as generated by NPs.

3.4.5 Visual MINTEQ simulations

When investigating environmental transformation of NPs, it is important take humic substances, HS, into consideration as they are a key component of NOM, as mentioned before. Therefore, modeling of their behavior when in contact with metal ions is of interest. There are some characteristics which complicates modeling, such as the heterogeneous binding sites for adsorption of HS onto metal ions or protons [83]. When it comes to acid-base properties concerning HS the most prominent sites in the pH range below 7 is carboxylic-acid-type groups and at higher pH phenolic-acid-type groups [84] [85].

The interactions between metal and NOM can occur due to several different mechanisms. In this study a specific surface complexation model, SCM, is used. This model is called the

Stockholm Humic Model, SHM. Here interactions are considered in three fundamentally different ways, as described below.

3.4.5.1 Adsorption isotherms
This method generally describes adsorption using empirical equations. This does not consider individual mechanisms, but rather uses common isotherm equations which are built in. However, the simplicity of these adsorption isotherms does limit the functionality of the model.

3.4.5.2 Ion-exchange reactions
This model considers ion-exchange reactions, which occur due to electrostatic (physical) attraction between a charged ion and a particle surface with opposing charges. To consider this ion-exchange Visual MINTEQ uses the Gaines-Thomas equation.

3.4.5.3 Surface complexation models
These models consider adsorption reactions for inorganic constituents which has a chemical contribution to the adsorption phenomena. Compared to the adsorption isotherms, this is done in a more thermodynamically correct way, commonly considering both physical and chemical electrostatic contributions of the adsorption process.

SCM:s often differ from each other in terms of describing electrostatic contribution to the surface of interest. As mentioned before, the model used for the simulations is the Stockholm Humic Model (SHM) [86].

3.4.5.3.1 Stockholm Humic Model
The SHM does a good job at describing the way metals and protons bind on to humic substances. The SHM model is based on several different model and assumptions. The main ones are the Basic Stern Model (BSM), discrete-site pK_a formalism and the impermeable sphere approach. The impermeable sphere approach views HS as impermeable spheres which assumes the charge to be located on the exterior part of the sphere. The discrete-site pK_a formalism is used to describe the pH dependence of proton binding [83]. This method assumes that a series of discrete pK_a values to the HS. Even if these values are discrete, the individual sites are not a physically representative of the present sites [85]. BSM is used as the interface model in SHM and is some, for the most part, empirical equation is included in order to handle the extra screening of charge [83]. Due to this it is capable to describe competitive interaction and metal binding over a variety of conditions.

4. Materials and methods

4.1 Particles

The Mn and Mn₃O₄ NPs were obtained from American Elements (Los Angeles, CA, USA), and had a specified the metal purity of 99.9%.

4.2 Dissolution experiments

4.2.1 Preparation

The solutions used in these experiments were a freshwater solution (FW) and another FW solution with an addition of natural organic matter (NOM). The FW solution contained 0.0065 g/L $NaHCO_3$, 0.00058 g/L KCl, 0.0298 g/L $CaCl_2 \cdot 2H_2O$ and 0.123 g/L $MnSO_4 \cdot 7H_2O$. After this the pH was adjusted to 6.2 to mimic natural FW condition. The NOM consisted of Suwannee River NOM, obtained by the International Humic Substances Society (USA).

The NOM solution was prepared by adding 1 mg of NOM (HA) powder to 0.1 M NaOH and thereafter mixing until dissolved, and then added to FW. The solution was left to equilibrate for a minimum of 24 h before adjustment of pH. PH adjustments were made using HNO₃. Approximately 30 μL of a HNO₃ with the concentration of 0,25 g/L was used to make 1 L of each solution.

A series of exposure experiments were performed to determine the ionic release of the nanoparticles. Mn and Mn₃O₄ NPs were exposed in two different mediums at 25 °C for 3 different durations of time. All exposures had 3 replicates and one blank. Some these experiments were repeated to ensure reliable results. This can be seen in Table 2 which summarizes the variations of exposure experiments.

Table 2. The repetitions of each exposure experiment. Each repetition consists of three samples and one blank.

	1h	2h	6h	24h
Mn with FW	1	-	1	1
Mn with FW and NOM	1	-	1	1
Mn_3O_4 with FW	4	-	2	3
Mn_3O_4 with FW and NOM	4	1	2	3

Figure 5 depicts a mixing schedule for the dissolution experiments, the mixing is divided into 8 steps. In step 1, the stock solution was made from adding 6 mL of MilliQ water to the powder which was measured beforehand. The concentrations of these initial stock solutions can be seen in Table 3. The stock solutions were continuously probe sonicated with an amplitude of 2, for 5 minutes. This corresponds to a delivered acoustic energy of 2400 J [87].

Dissolution experiments

Take out 1.4 mL

8 — Dilute to 7 mL with MilliQ. Acidify, treat with King's water, then analyse with AAS

Take out 1 mL for NTA.

Dilution 1:100:
100 µL stock into 9.9 mL FW+ NOM (or FW)

Dilution:
1.4 mL into 5.6 mL FW+ NOM

3 mL from supernatant

Take out 4 mL

1 h

1

6 mg nanoparticles
In 6 mL MilliQ
Sonication:
• Continous
• Amplitude=2
• Time= 5min

2

FW + 10 mg/L
Suwannee river
NOM (or just FW)

3 — Expose 1/6/24 h → 4

FW + 10 mg/L
Suwannee river NOM
pH 6.2
Triplicate samples and one blank

Ultracentrifugation
for 1h at 50000
rpm.

5

Meaure pH.
Acidify to pH<2

Dilute 1:10 in MilliQ:
1 mL stock + 9 mL MilliQ

6 → 7 → AAS analysis

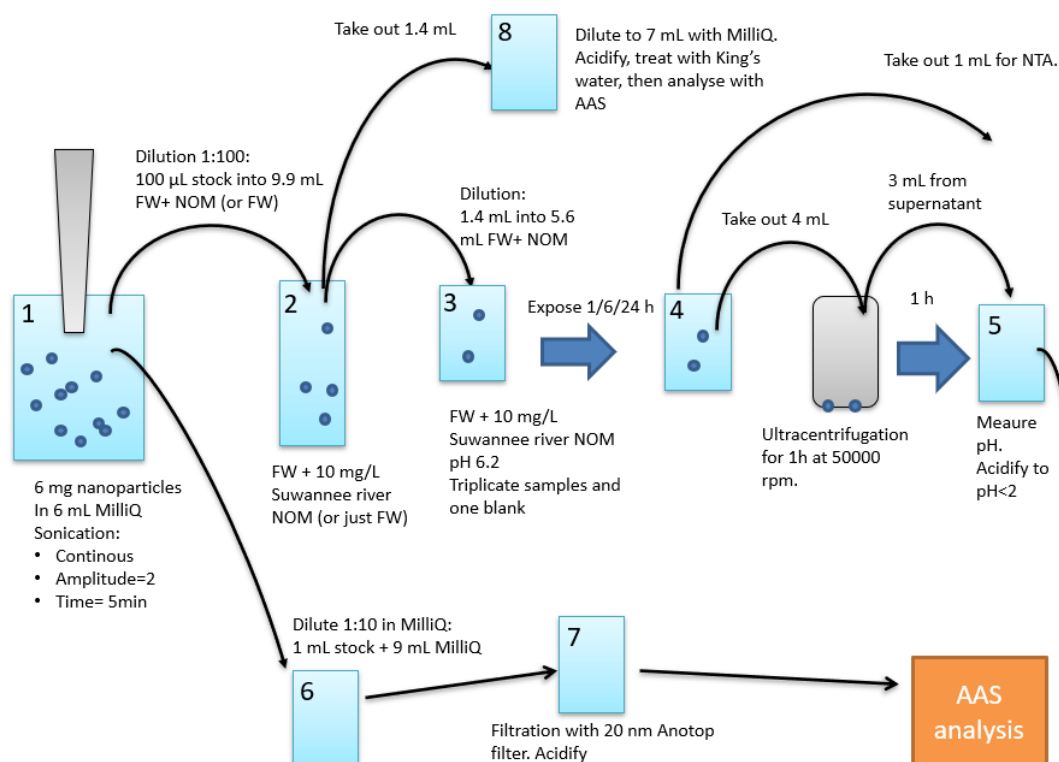Filtration with 20 nm Anotop filter. Acidify

Figure 5. illustration of the preparation of samples for investigating the dissolution of the NPs.

The samples in one experiment were diluted from the same stock solution, but the stock solution slightly varies for the different experiments. This is because every stock solution is required to be prepared in conjunction with the experiment to reduce the amount of ion release before the exposure. The concentration of the different stock solutions can be seen in table 3.

Table 3. The original concentration of each stock solution used to prepare each sample. This is calculated from the original weighing of the powder. In order to get approximately the same amount of Mn for both types of particles the weights between the samples containing Mn and Mn_3O_4 are different. Batch one is noted as B1, batch two as B2 and so on.

	1 h	2h	6 h	24 h
Mn with FW	1.007 g/L	-	1.006 g/L	1.009 g/L
Mn with FW and NOM	1.003 g/L	-	1.005 g/L	1.009 g/L
Mn_3O_4 B1 with FW	1.444 g/L	-	1.453 g/L	1.443 g/L
Mn_3O_4 B1 with FW and NOM	1.447 g/L	-	1.432 g/L	1.451 g/L
Mn_3O_4 B2 with FW	1.429 g/L	-	-	1.371 g/L
Mn_3O_4 B2 with FW and NOM	1.377 g/L	-	-	1.390 g/L
Mn_3O_4 B3 with FW	1.422 g/L	1.389 g/L	-	-
Mn_3O_4 B3 with FW and NOM	1.419 g/L	-	-	-
Mn_3O_4 B4 with FW	1.427 g/L	-	1.409 g/L	1.386 g/L
Mn_3O_4 B4 with FW and NOM	1.435 g/L	-	1.385 g/L	1.454 g/L

In step 2, the stock solution was diluted with 9.9 mL of ether NOM or pure FW solution depending on which experiment was made. In step 3, the samples were prepared for exposure. The samples made for exposure were triplicates and there was also one blank which underwent the same exposure. The triplicates were prepared by adding 1.4 mL of the solution from step 2 to beakers which contained 5.6 mL of ether the NOM or FW solution, depending on which of there were examined. The blank was just 7 mL of ether the NOM or FW solution. Three of these were replicates and the blank were exposed for ether 1. 6 or 24 h in a chamber with a temperature of 25 ℃. In step 4 the samples were prepared to be centrifuged after the exposure had ended by adding 4 mL of each sample into test tubes which fits in the centrifuge and can withstand being centrifuged. The samples were centrifuged for 1 h at 50000 rpm. In step 4, 1 mL from each sample were also taken out separately to use for NTA analysis. In step 5, 3 mL of the supernatant from the samples were transferred into new beakers and was acidified using concentrated HNO_3. These four samples were later analyzed using AAS.

In step 6 one mL the stock solution from step 1 was diluted into 9 mL of MilliQ water. In step 7 this suspension was immediately filtered 20 nm pore size filter (Anotop, Whatman) and later acidified using concentrated HNO_3. This was done to determine how much of the particles were dissolved before exposure.

In step 8, 1.4 mL of the solution from step 2 was added to 5.6 mL MilliQ water. After this the samples were acidified using concentrated HNO_3. To ensure that the particles were completely dissolved it was also treated with Aqua Regia before AAS analysis. The purpose of this step was to measure the total concentration of Mn in the samples. This samples were later used as a reference to the exposed samples to be able to se how much Mn was realised during exposure.

Total concentration samples as well as the exposed samples were diluted 1:400 while the sample which is filtrated immediately only is diluted 1:10 from the stock solution.

4.2.2 AAS

The instrument used for these analyses was a Perkin Elmer AAnalyst 700. This is a GF-AAS which has both flame and heated graphite furnace atomizers(HGA). [88] Firstly, a calibration was performed with containing known concentrations of manganese ions from a certified standard (Perkin Elmer), to ensure accuracy.

After this the samples were added into cuvettes and all the regular samples (supernatants from centrifuged, exposed solutions) were diluted 1:10 while the filtered ones were diluted 1:20. If any sample had concentrations outside the calibration range, these samples were diluted further and reanalyzed by the AAS instrument. All values were then recalculated to be comparable to the concentration of the samples obtained in step 4.

When analyzing the total concentration samples, from step 8, all particles in the sample needed to be fully dissolve. Therefore, these samples were treated with aqua regia before analysis so ensure full dissolution. Here 8 ml Aqua Regia was added to the samples which contained 7 ml originally. Before adding Aqua Regia this method was tested on other samples with a known concentration to make sure everything would dissolve properly and give an accurate reading during AAS measurement.

These test samples were made from the same Mn and Mn_3O_4 nano powder used in the dissolution experiments which are described above. From this powder 8 samples were made, 4 with the Mn and 4 with the Mn_3O_4 powder. The concentration for these samples was known beforehand by weighing the powder and adding a known volume of Aqua Regia to the powders. These samples were then analyzed using AAS. In table 4 the concentration using AAS is divided with the calculated concentration.

Table 4. The results from the test samples used to evaluate the robustness of the method used to fully dissolve the total concentration samples.

Mn 1	81 %
Mn 2	82 %
Mn 3	76 %
Mn 4	83 %
Mn_3O_4 1	108 %
Mn_3O_4 2	82 %
Mn_3O_4 3	103 %
Mn_3O_4 4	100 %

To test the accuracy of the AAS a few samples using a known concentration of Mn ions was used. These all came back with very high accuracy.

4.3 NTA

While preparing the dissolution experiments, just before the samples were put in the ultracentrifuge, one ml of the samples each were removed to run NTA, as seen in Figure 5. Here the instrument was first calibrated with a liquid containing silica particles of known particle sizes before running any tests. Five measurements were taken which each lasted for 60 seconds for each sample. The temperature was also set to be 25 °C for all samples. These measurements were collected by using a syringe to push a new part of the sample forward to a new random location. However, during measurements no new amounts of sample were pushed forward. These five tests were later combined to one average which was plotted.

When running the NTA the camera level was set to be 8 for the Mn NPs and 4 for the Mn_3O_4 NPs. The selectivity threshold was chosen to be 7 for the Mn NPs and 6 for the Mn_3O_4 NPs. The sensitivity threshold can be set manually, and it controls how sensitive the software is when identifying what is and is not a particle during measurement.

4.4 ATR-IR

The instrument used in these measurements was a Bruker Tensor 37 FT-IR spectrometer. This instrument can handle liquid samples and has a spectral range of 7500 to 370 cm^{-1}. [89]

Samples of approximately 15 mg of powder, Mn or Mn_3O_4, and 6 ml ethanol were prepared and sonicated (similar settings as for dissolution investigations). This solution was added dropwise onto the ATR crystal. When one drop has dried another was added. This was repeated 20 times until a thin film of particles were formed. The film was then left to dry for another two hours before the measurement was performed. First, a background was recorded, if NOM solution was tested the background was taken with FW and if a FW solution was tested it was taken with MilliQ water. After this, the film was exposed to the solution of interest and a spectrum was recorded every fifth minute for between 2-5 hours and then examined. Lastly, after these measurements were taken, approximately 8 ml of the solution, same as the background, were flushed trough the detection chamber which

contains the NP film. This was done to see if the components which may have adsorbed onto the NPs would loosen.

4.5 ROS

4.5.1 DCHF Preparation

The starting solution was DMSO with 10 mM of DCFH-DA added. 5 µL of this solution was mixed with 0.4 mL of an 0.01 M NaOH solution. This was done twice since different media, FW, and FW with NOM, were investigated. These mixtures were left on ice in darkness for 30 min on order to react and form DCFH. After this the pH was neutralized by adding 2 ml of their respective medias. Next the pH was set using 0.025 M HNO_3 and after this the mixture was left on ice in darkness until use. The pH for the FW-DCFH solution was 6.24 and the pH for the FW-NOM-DCFH solution was 6.21.

4.5.2 Particle suspension preparation

The Mn and Mn₃O₄ particle suspensions were prepared by first weighing and dividing the powders into 4 samples, two with Mn and two with and Mn_3O_4. These samples contained 3 mg each. 3 ml of MilliQ water was added to all the samples creating 4 stock solution with an approximate particle concentration of 1 g/L.

The solutions were sonicated for 10 minutes two times. In between sonication the solution was vortexed for 10 s. After this the 600 μL of either FW or FW with NOM media were added to the stock solutions, which diluted the suspensions to a concentration of 0.4 g/L NPs. This resulted in four different particle suspensions: Mn-FW, Mn-NOM, Mn₃O₄-FW, and Mn₃O₄-NOM. The samples were then vortexed for another 10 s each before measurement.

4.5.3 Measurement

To measure the fluorescence an Infinite F200 PRO multimode plate reader from TECAN, Austria was used. The excitation wavelength was set to 485 nm and the emission wavelength to 535 nm.

The measurement was performed using a plate with 96 wells in which liquid could be added. When testing all four particle suspensions (Mn-FW, Mn-NOM, Mn₃O₄-FW, and Mn₃O₄-NOM) two blank samples were also added which contained pure FW and FW with NOM. All 6 combinations were tested as quadruplicates with 75 μL DCFH-media solution and 25 μL particle suspension (see above), or just medium for the blanks, in each well, resulting in 24 wells when the blanks are included. This means that each well contained 0.015 mM DCFH-DA, 1.2 mM NaOH, 0.27 mM DMSO and 100 mg/L NPs.

The fluorescence was measured every fifth minute for one hour using the plate reader. The results were later divided with their respective blanks to retrieve the increase.

4.6 Visual MINTEQ

Visual MINTEQ Version 3.0 was used for the metal speciation simulations [90]. The output of the program gives is a list of compounds which the manganese ion has bounded to in the solution. From this it is possible to see which forms and how the Mn is distributed and therefor also how much of it has complexed the NOM.

To start with, all the different elements which are included in the FW solution were added, see Table 5. The concentrations were set so that they mimicked the experimental concentrations used in the dissolution experiments. The same was done when adding NOM to the simulation, with NOM defined as fulvic acid. The concentration of Mn ions was varied 6 times for the 2 different simulations. The concentrations used was 0.05 mg/L, 0.2 mg/L, 0.25 mg/l, 0.3 mg/L, 0.4 mg/L and 1 mg/L of Mn ions.

Table 5.The different components used in the simulation.

Component name	Total concentration [Molal]
Na^+	0.0000747
CO_3^{2-}	0.0000747
K^+	$7.79 * 10^6$
Cl^-	0.00046
Ca^{2+}	0.000228
SO_4^{2-}	0.0000499
Mn^{2+}	*Varied*
Mn^{3+}	0
NOM	0.000116

After adding all the components, the Stockholm Humic Model, SHM, was chosen as the adsorption model for the simulation, the pH was fixed at 6.2 and the temperature at 25 °C. The redox potential was set to 300 mV, which is a relavant potential for FW environments. All compounds containing Mn was added to the list of possible species which makes them possible to form during the simulation but will not necessarily do so if it is not favorable for the systems. One redox couple was also chosen which was Mn^{3+} and Mn^{2+}.

5. Results

5.1 Dissolution of nanoparticles

Figure 6 presents the dissolution of Mn NPs in FW and FW with NOM. As seen in Figure 6 an increase in released Mn species to solution was observed when increasing the exposure time for both FW and FW with NOM. This trend was more prominent for the solution which did not contain any NOM. Student's t-test were performed for all three exposure times to investigate possible statistically significant differences between the samples which contained NOM compared to the ones that did not($p < 0.05$). No significant difference was found for the 1 h and 6 h exposure, but the 24 h samples were shown to be significantly different between FW and FW with NOM. This indicates that the dissolution was generally lower in the presence of NOM.
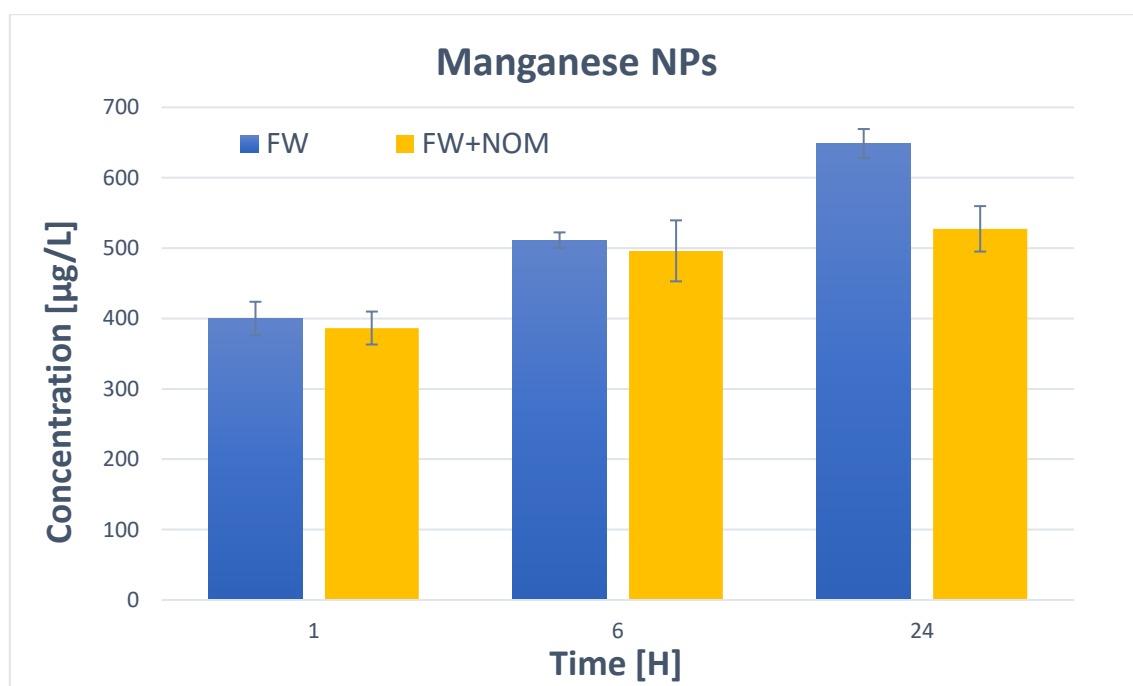
Figure 6. Release of Mn from Mn NPs in FW and FW with NOM. The exposures were performed at pH 6.2 at 25 °C.

In Figure 7 the data in Figure 6 has been divided with the value of the corresponding total concentration samples (Sample 8 in Figure 5). Figure 7 therefore show how much of the sample has dissolved compared to its original concentration. In this figure the dissolution seems to be a bit larger when NOM is present. Also, here the dissolution is the largest for the 6 h samples instead of the 24 h ones which has the second largest dissolution in Figure 6. A significant difference can be seen between the FW and FW & NOM solution for the following exposure times; 1 h, 6 h and 24 h.
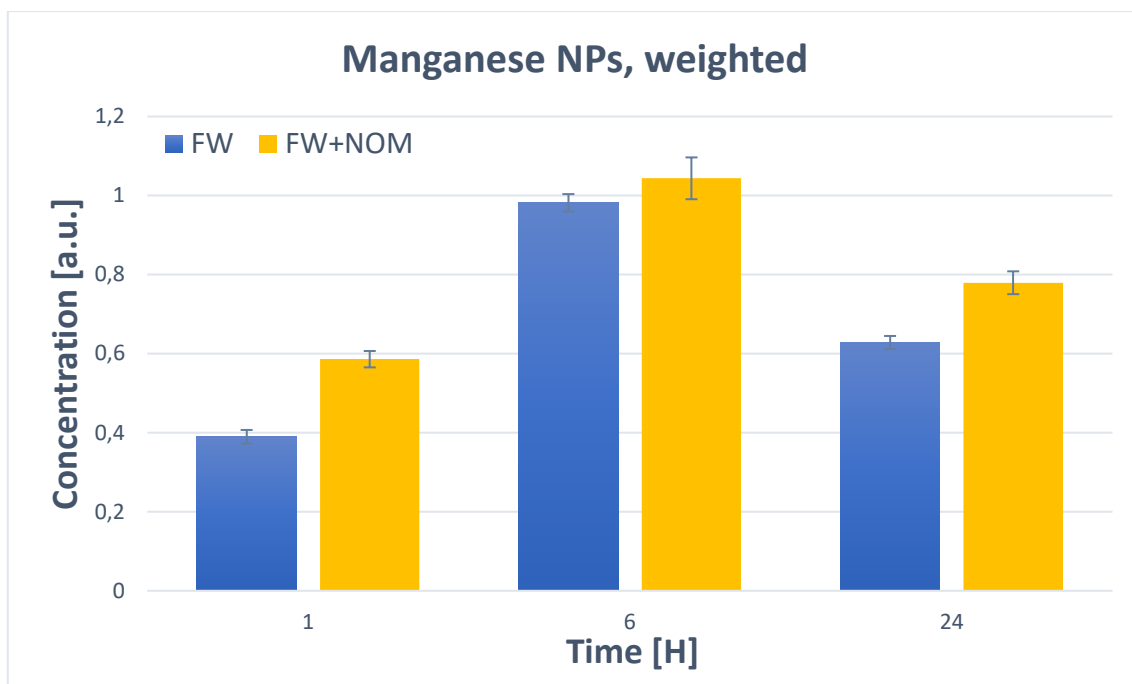
Figure 7. Release of Mn from Mn NPs in FW and FW with NOM, normalized to the total Mn concentration added to the exposure.

More than one test batch was performed for the Mn_3O_4 NPs. This was because the results were considered as questionable due to very large dissolution for 1 h in FW for batch 1, and also contradicting trends were found between batch 1 and 2. It was also not expected that the Mn concentration for the Mn_3O_4 NPs to decrease over time since the Mn NPs did not showcase this. Therefor additional testing was required. The results from the different batches were quite varied and did not show a clear trend, se Figure 8.

As seen in Figure 8 the amount of dissolved manganese for batch 1 decreased when the exposure time increased. In some of the Mn_3O_4 NPs samples in batch 1 the amounts of dissolved manganese were quite high. In batch 1 the amount of Mn is significantly larger in the solution which contains only FW compared to the one which has NOM.
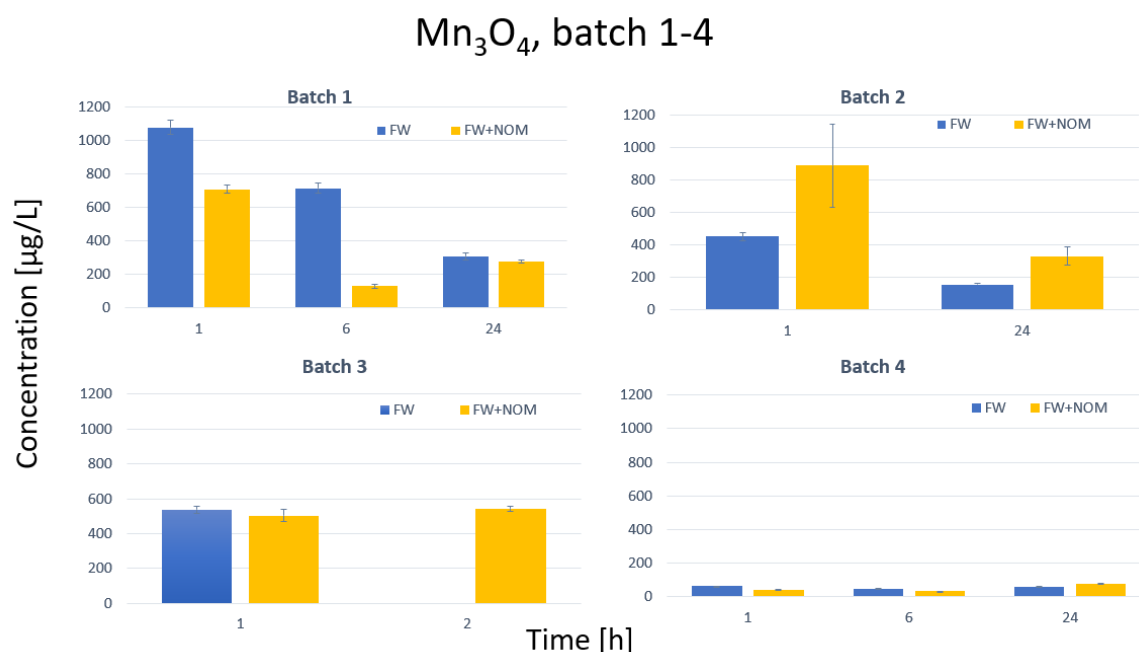
Figure 8. Release of Mn from Mn₃O₄ NPs in FW and FW with NOM. Batch 1-4.

Figure 9 shows that manganese release normalized to total concentration. There were some differences between Figure 8 and 9, when viewing batch 1. The values of the samples with FW solution are still higher than those with NOM in Figure 8 but this gap is not as large as seen in figure 9.

As seen in Figure 8 and 9, batch 2 was different from batch 1. Here, the NOM solution initially showed a higher Mn concentration compared with FW only. However, when for the samples which were exposed for 24 h, the values were close to the ones in batch 1 with the exception that the one that did not contain NOM had a slightly lower value in batch 2. When preforming Student's t-tests, on the values from figure 8, significant differences between the NOM and FW batches were found for the following exposure times; 6 h exposure in batch 1, the 1 h and 24 h exposure in batch 2, the 1 h exposure in batch 3, and the 1 h and 6 h exposure in batch 4.

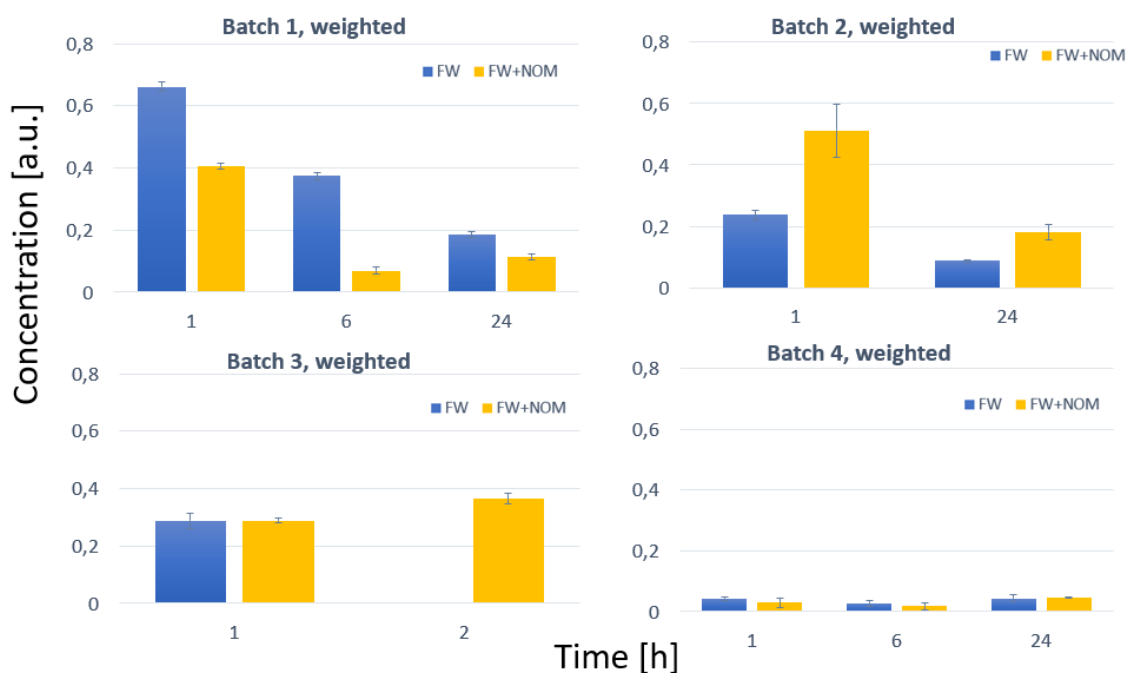# Mn$_3$O$_4$ – dissolution normalized to total concentration, batch 1-4

Figure 9. Release of Mn from Mn$_3$O$_4$ NPs in FW and FW with NOM normalized to the total concentration added to the exposure. Batch 1-4.

In difference to batch 1 and 2 the concentration of Mn seems to not decrease in batch 3 after longer exposure, which the t-tests suggests as well. The dissolution in batch 4 was largest at 24 h, followed by the 1 h. The Mn$_3$O$_4$ NPs dissolved more in FW than FW+NOM, except for 24 h. The dissolution was also drastically lower in batch 4 compared to the other batches, here it is almost a tenth of the previous batches.

In figure 10-11 the values for the total concentration tests can be seen on their own. Note that for each kind of NP, Mn or Mn$_3$O$_4$, the values are expected be quite similar. Mostly, this aligns with the results but there are a few exceptions such as Mn-FW-1 h, Mn-FW-24 h. For the Mn$_3$O$_4$ NPs fluctuation from around 1350-1900 µg/L were common.
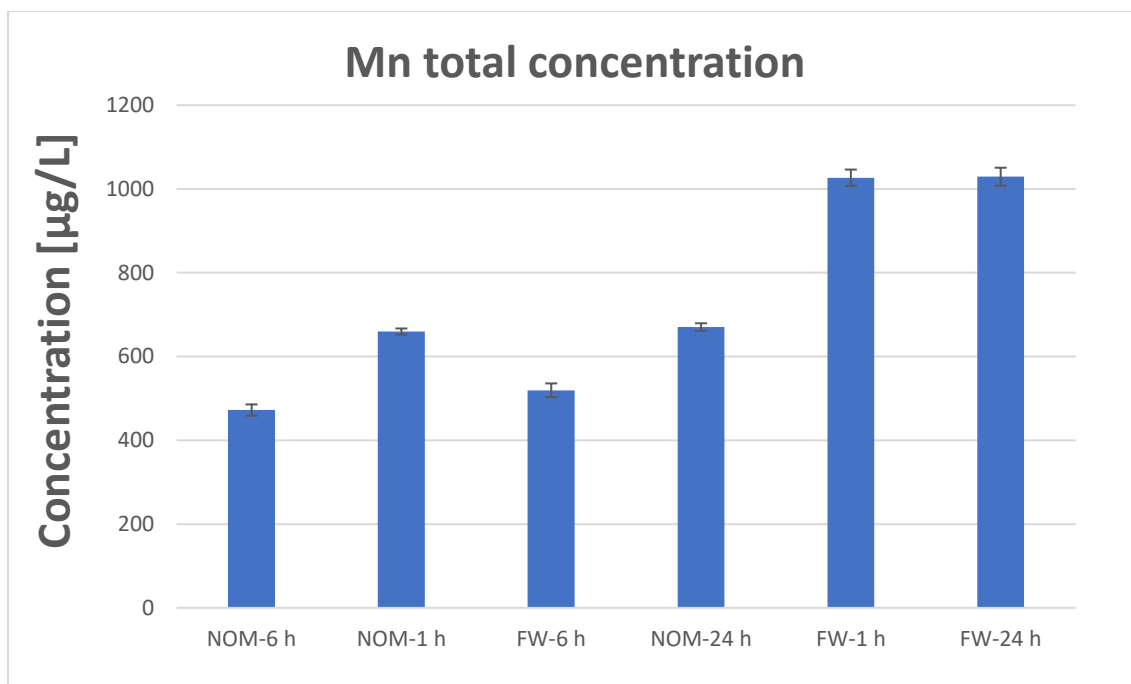
Figure 10. The results from the total concentration tests on the Mn NPs.
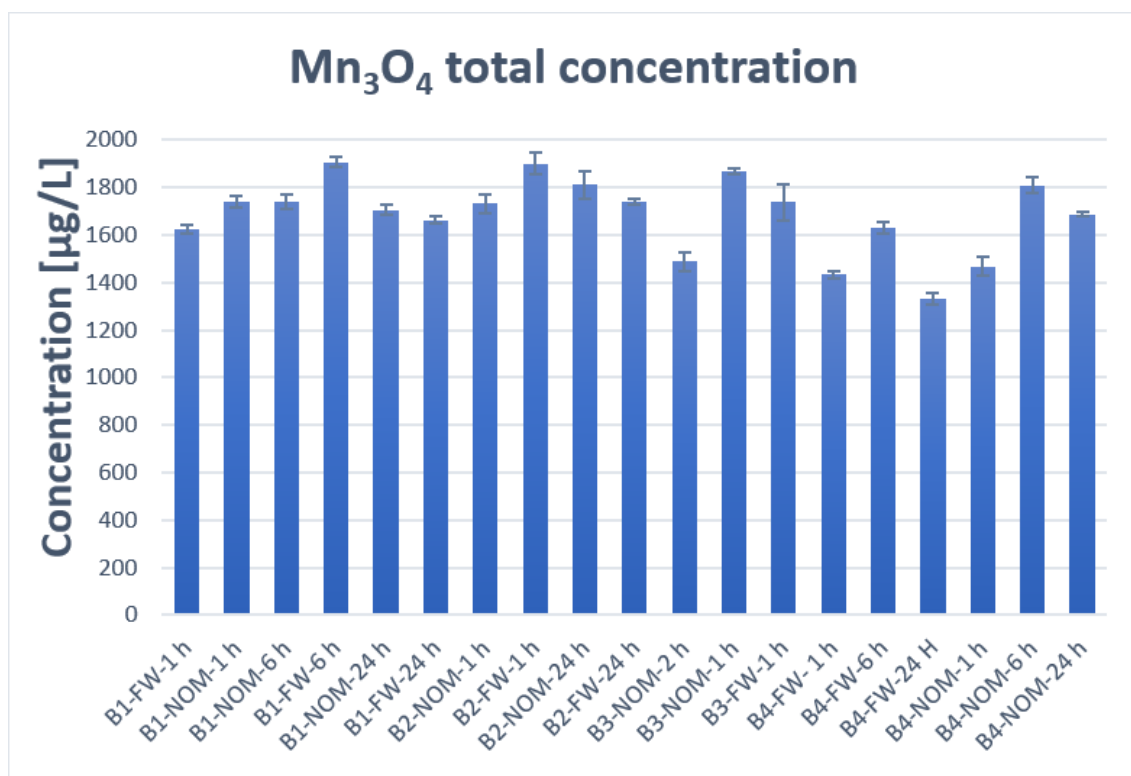

Figure 11. The results from the total concentration tests on the Mn₃O₄ NPs.

5.1.1 Dissolution in stock solutions

The dissolution taking place during the sonication step was investigated, as seen in step 6-7 in Figure 5, as it has been shown that relatively reactive metallic NPs will to some extent dissolve during the dispersion preparation. [87] Therefore, samples were collected and filtered directly from the stock solution after sonication. The Mn concentrations were relatively similar for all samples. For Mn the mean value for the initial dissolution was 38 µg/L, or 5.2%, (see Figure 12).
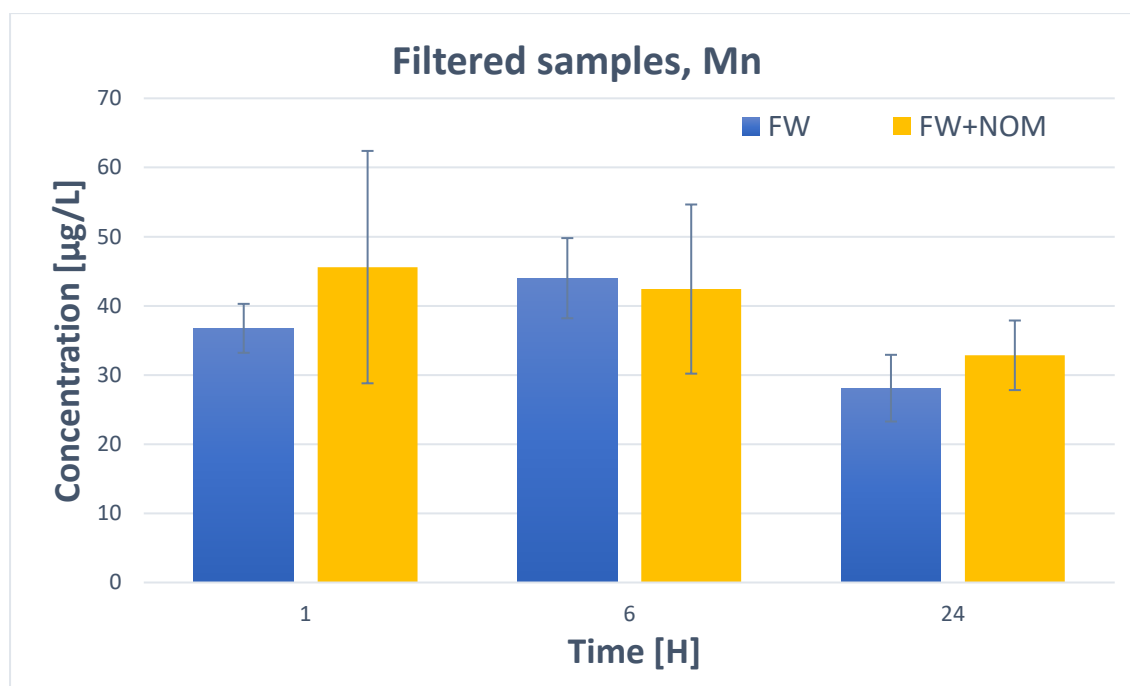
Figure 12. Dissolved Mn as measured directly after sonication for Mn NPs, before exposure in FW or FW and NOM. The samples were filtered with 20 nm pore size filters.

The initial dissolution from each batch of Mn_3O_4 NPs can be seen in Figure 13. In batch 1 the sample from the FW-6 h had an unusually high standard deviation and is therefore unsuitable to be used as comparison to the other samples. Other than this, the samples containing Mn_3O_4 NPs were also quite similar, except for batch 2-NOM-1 h, which raises the mean value a bit. The mean value was 21 µg/L, which means that the oxide form of manganese NPs had a slightly lower dissolution in the stock solutions compared to the Mn NPs.
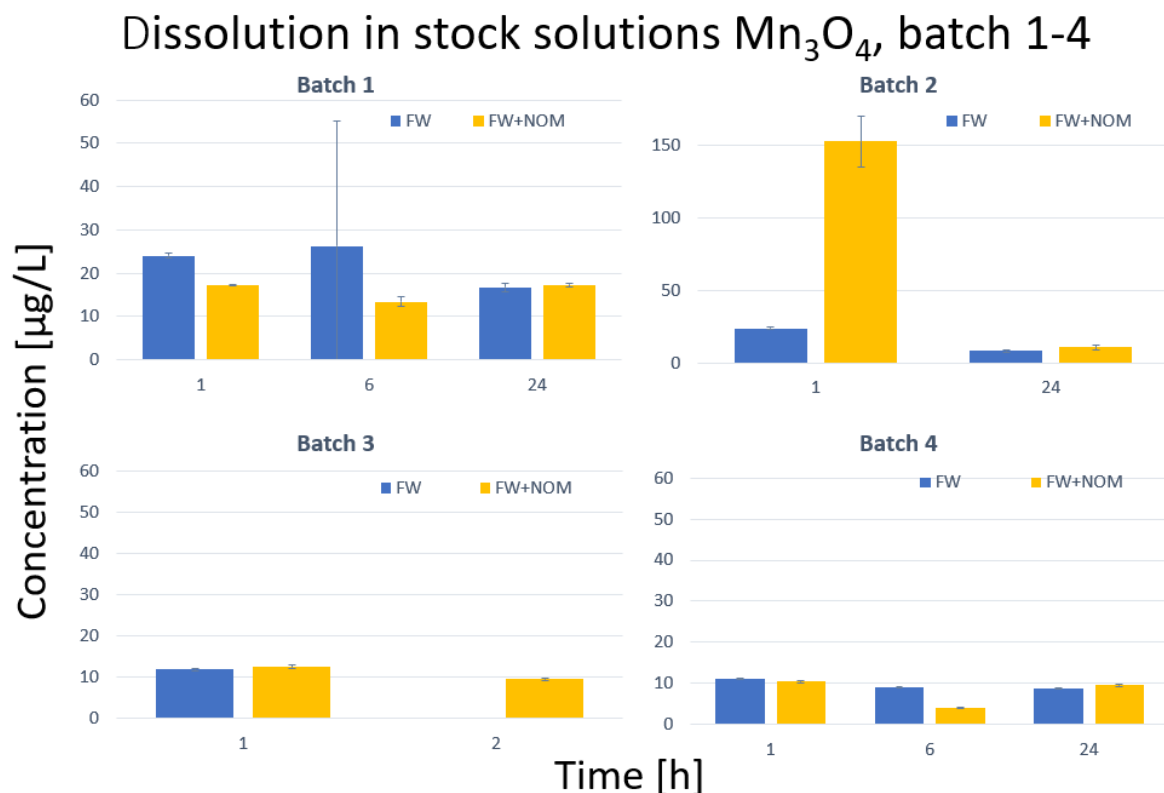
Figure 13. Dissolved Mn as measured directly after sonication for Mn₃O₄ NPs, before exposure in FW or FW and NOM.

5.2 NTA

NTA was only preformed for batch one of the Mn and Mn_3O_4 NPs, resulting in 12 samples in total.

All the tests which were tested with NTA had large standard deviations between the replicas. This is likely to be because the concentrations of the NPs in all the tests were very low which means that the particles that did show in the test were very few and quite diverse in size. There also likely to be some agglomeration and sedimentation which will affect the number of particles in the suspension as well. The blanks tested showed a lot lesser amounts of particles compared to the samples, with some weak signals originating from NOM agglomerates.

In the Figure 14 and example where the standard deviation is included is shown using Mn_3O_4-24 h, but this is representative for all samples. As seen in Figure 14 the standard deviation is very large in comparison to the obtained particle sizes. Due to this it is hard to draw reliable conclusions from any of the particle concentration NTA data.
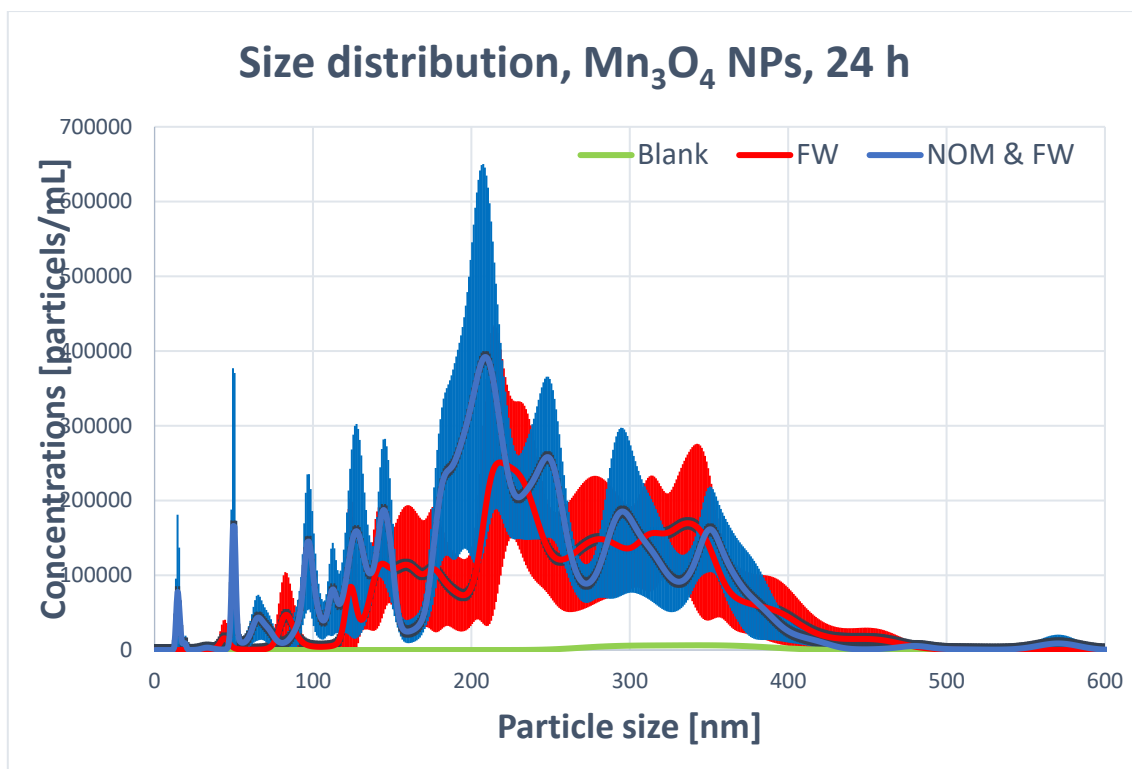
Figure 14. Size distribution of Mn₃O₄NPs after 24 h. The black area represents ± one standard deviation of the NOM+FW samples (3 replicas) while the blue area represents ± one standard deviation for the FW sample (3 replicas).

5.2.1 Manganese NPs

Generally, all the Mn NPs which contained NOM seemed to show a higher number of larger particles compared to the ones who did not. This can be seen in Figure 15-17. However, due du the large standard deviations it is hard to confirm this. The blank samples were also very low which is expected since they did not contain NPs.
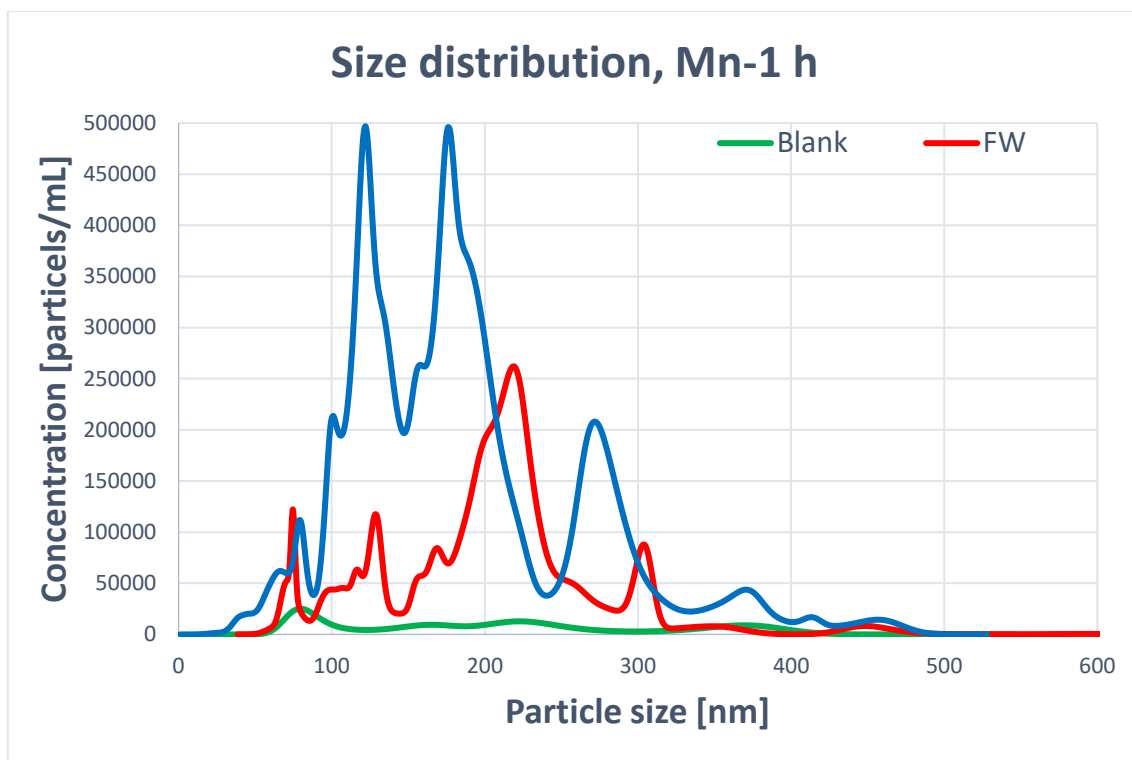
Figure 15. NTA results for size distrubutions of Mn NPs exposed with and without the addition of NOM, after 1 h exposure. The blank is the FW+NOM solution without particles.
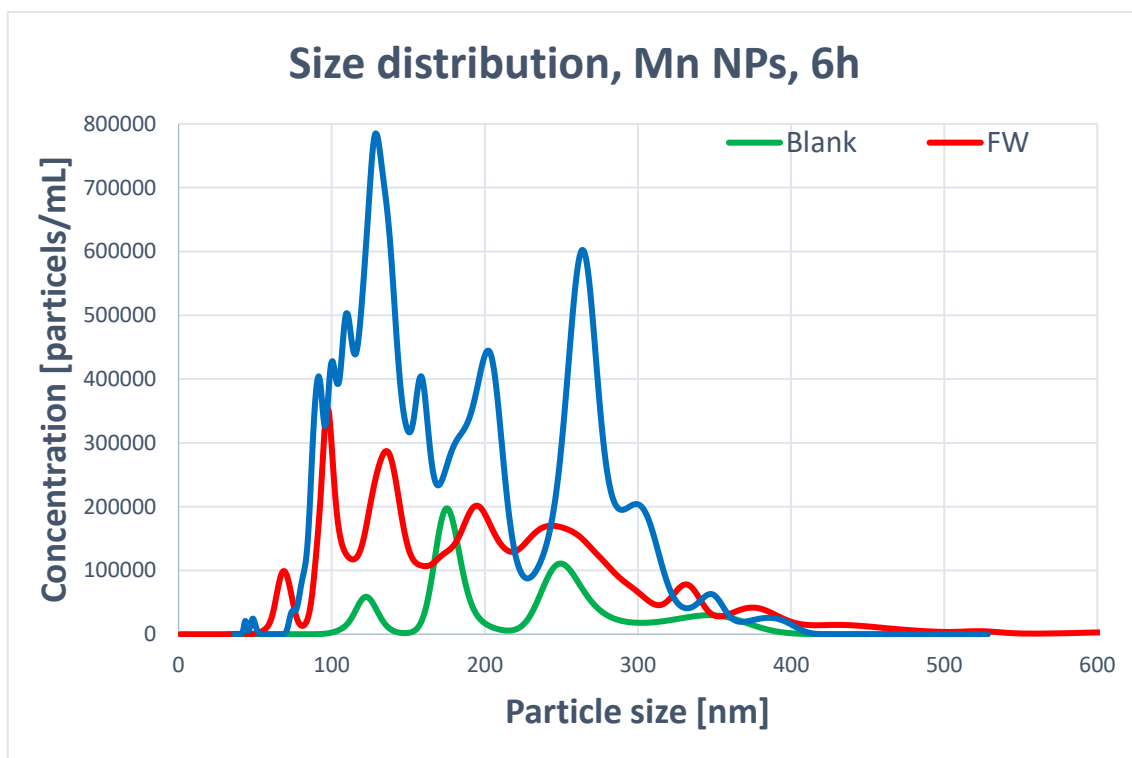

Figure 16. NTA results for size distrubutions of Mn NPs exposed with and without the addition of NOM, after 6 h exposure. The blank is the FW+NOM solution without particles.
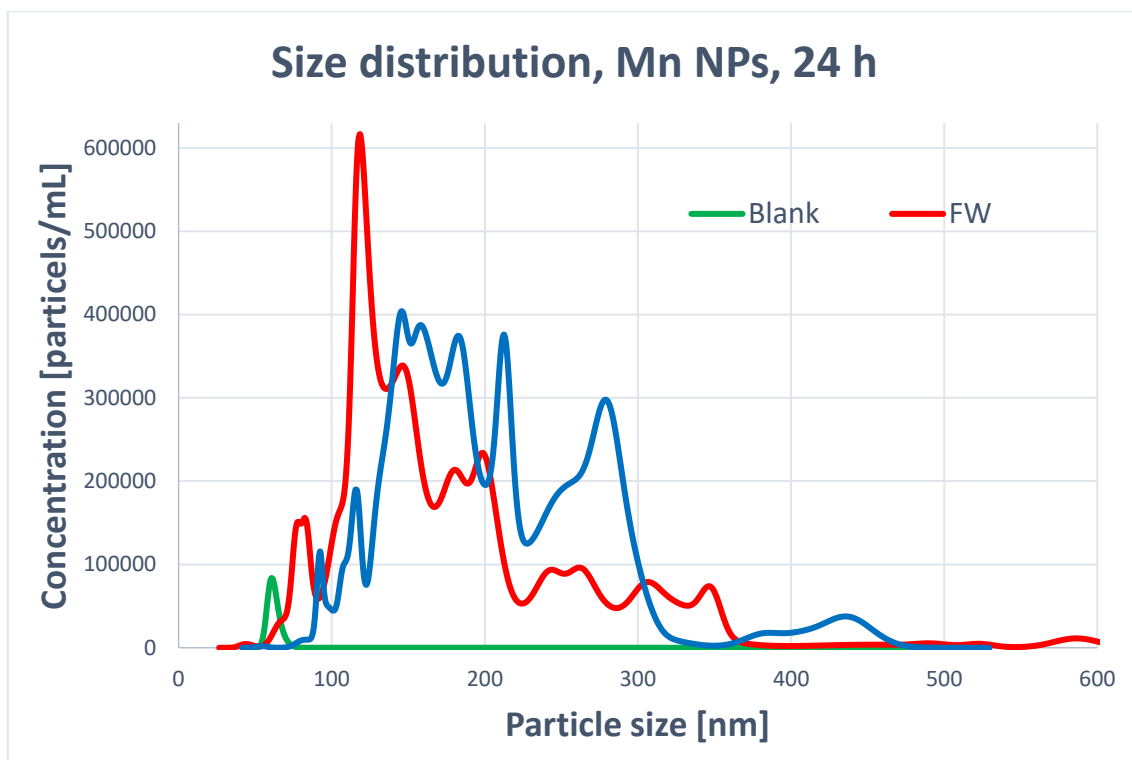
Figure 17. NTA results for size distrubutions of Mn NPs exposed with and without the addition of NOM, after 24 h exposure. The blank is the FW+NOM solution without particles.

5.2.2 Manganese oxide NPs

Figures 18-20 shows the size distributions for Mn_3O_4 NPs in FW and in FW with NOM. Here, no clear difference can be seen for Mn_3O_4 NPs for when they are suspended in FW or FW with NOM. Here as well, the blanks showed a much lower signal compared to the other samples, as expected.
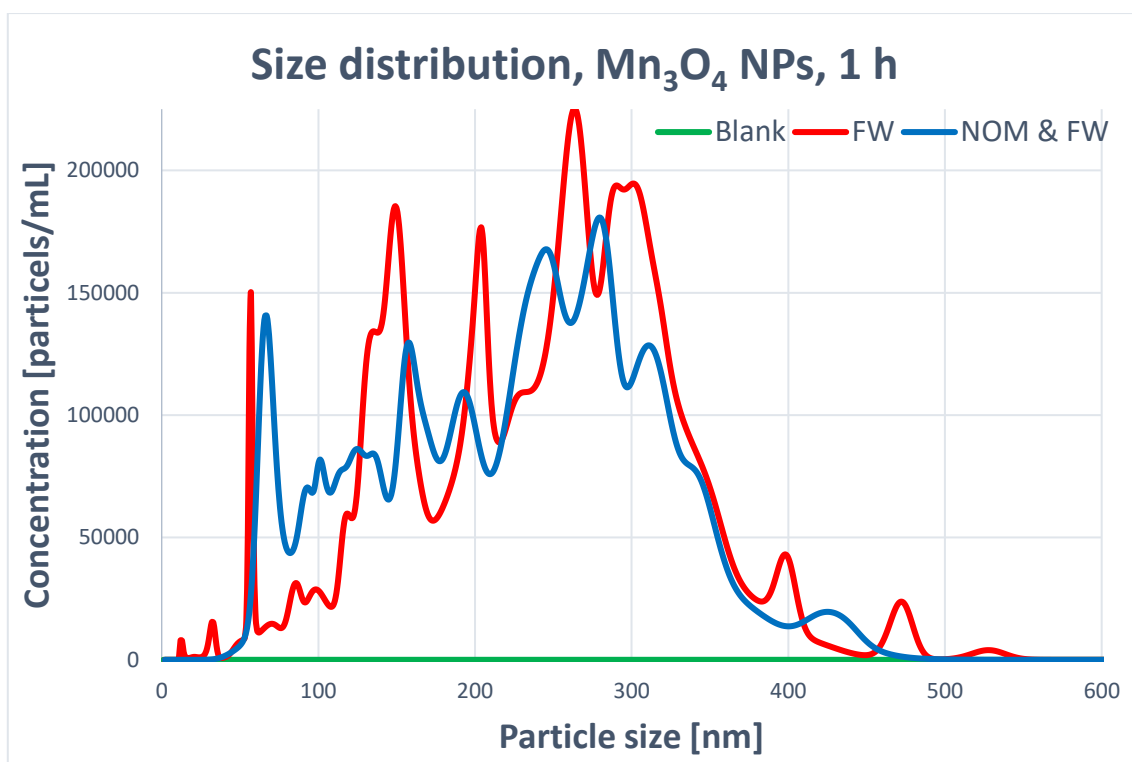
Figure 18. NTA results for size distrubutions of Mn₃O₄ NPs exposed with and without the addition of NOM, after 1 h exposure. The blank is the FW+NOM solution without particles.

Figure 19. NTA results for size distrubutions of Mn₃O₄ NPs exposed with and without the addition of NOM, after 6 h exposure. The blank is the FW+NOM solution without particles.

Figure 20. NTA results for size distrubutions of Mn₃O₄ NPs exposed with and without the addition of NOM, after 1 h exposure. The blank is the FW+NOM solution without particles.
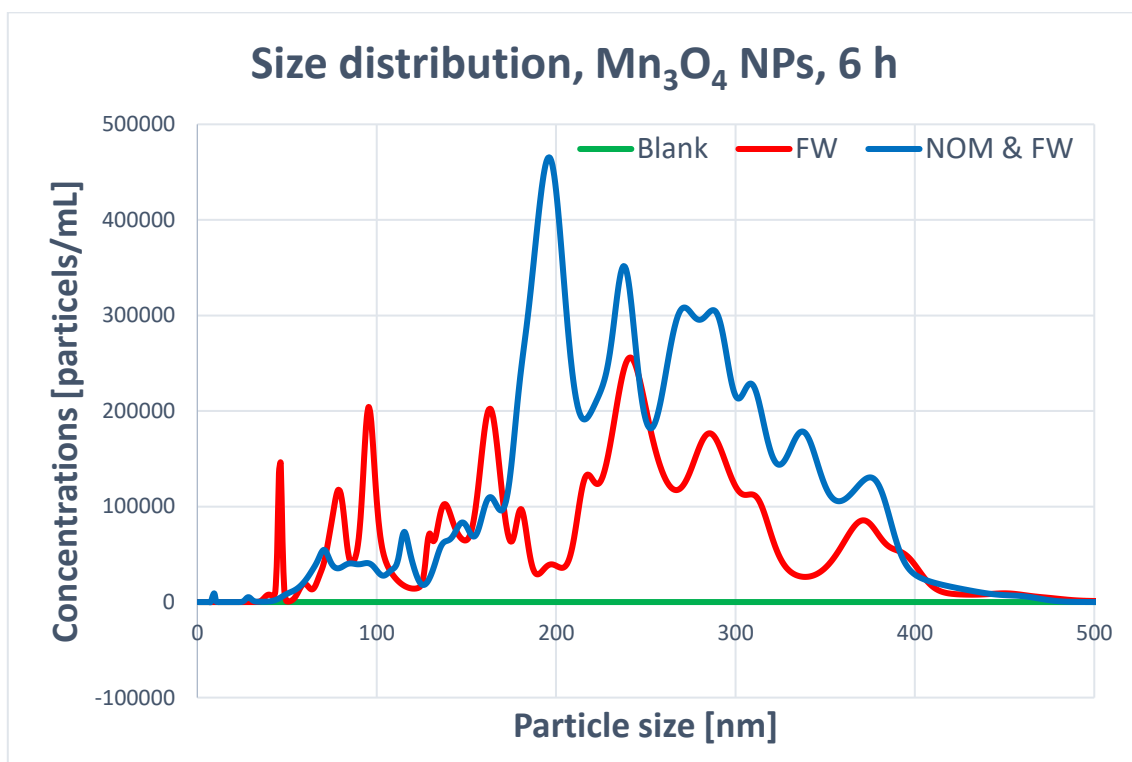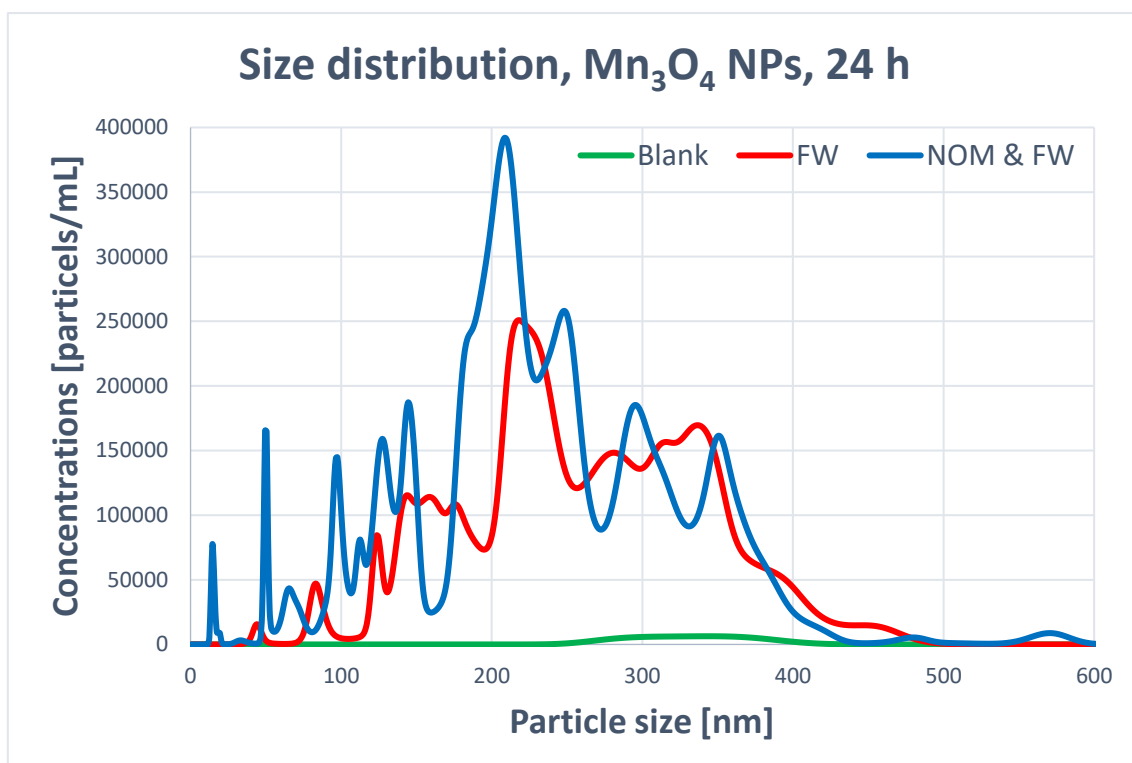
5.3 ATR-IR

The duplicated ATR-FTIR spectra of Mn NPs in FW with NOM are displayed in Figure 21 and 22. In these peaks were seen at approximately 1060, 1100, 1385, 1565 and 1730 cm^{-1}.
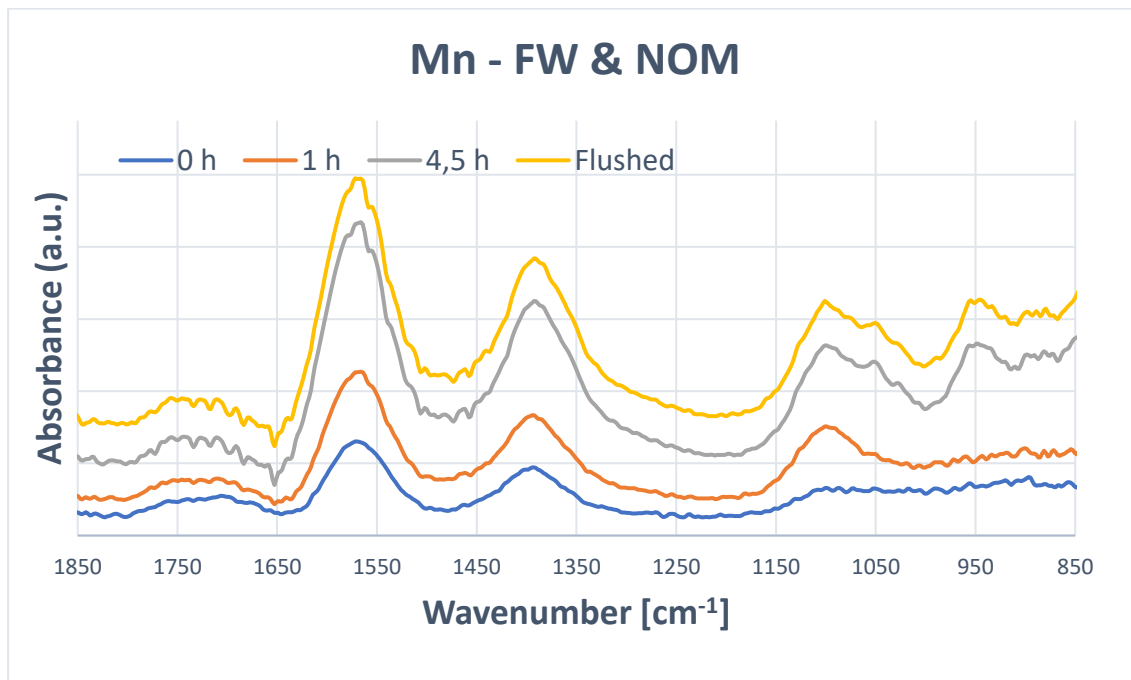

Figure 21. ATR-FTIR spectra of Mn NPs in FW with added NOM. Peaks can be seen at 1100, 1398, 1575, and 1730 cm^{-1}.
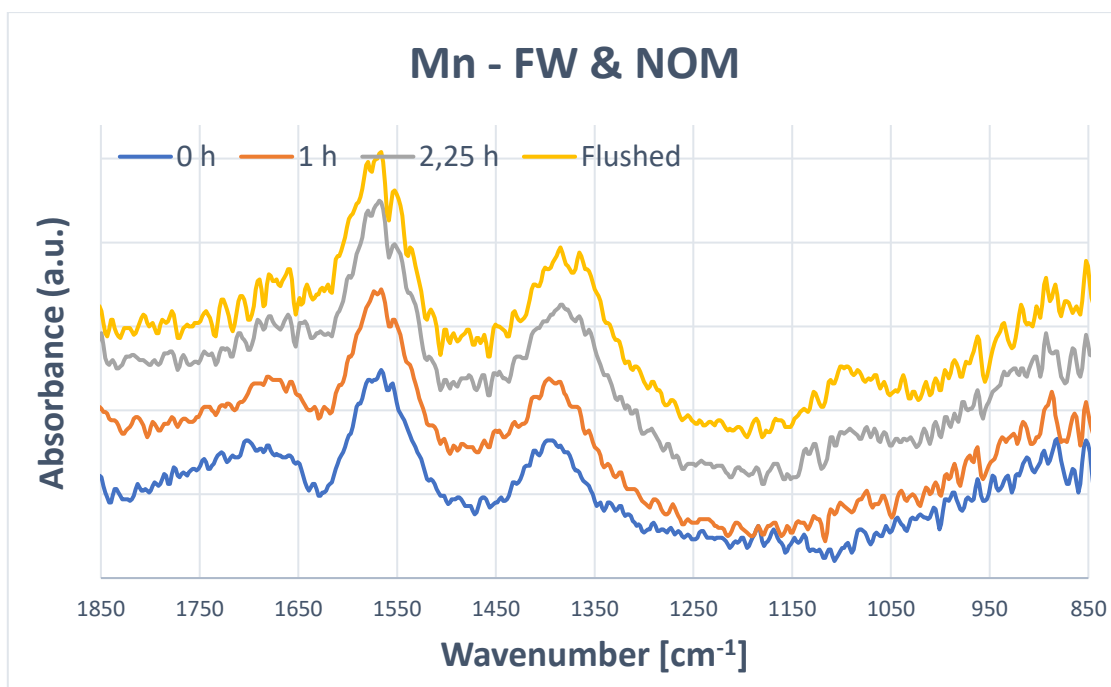
Figure 22. ATR-FTIR spectra of Mn NPs in FW with added NOM. Peaks can be seen at 1100, 1388, 1577, and 1689 cm^{-1}.

In Figure 23 and 24 the spectrums for Mn NPs films without NOM is shown. These had peaks around 1100, and 1385 cm^{-1}.
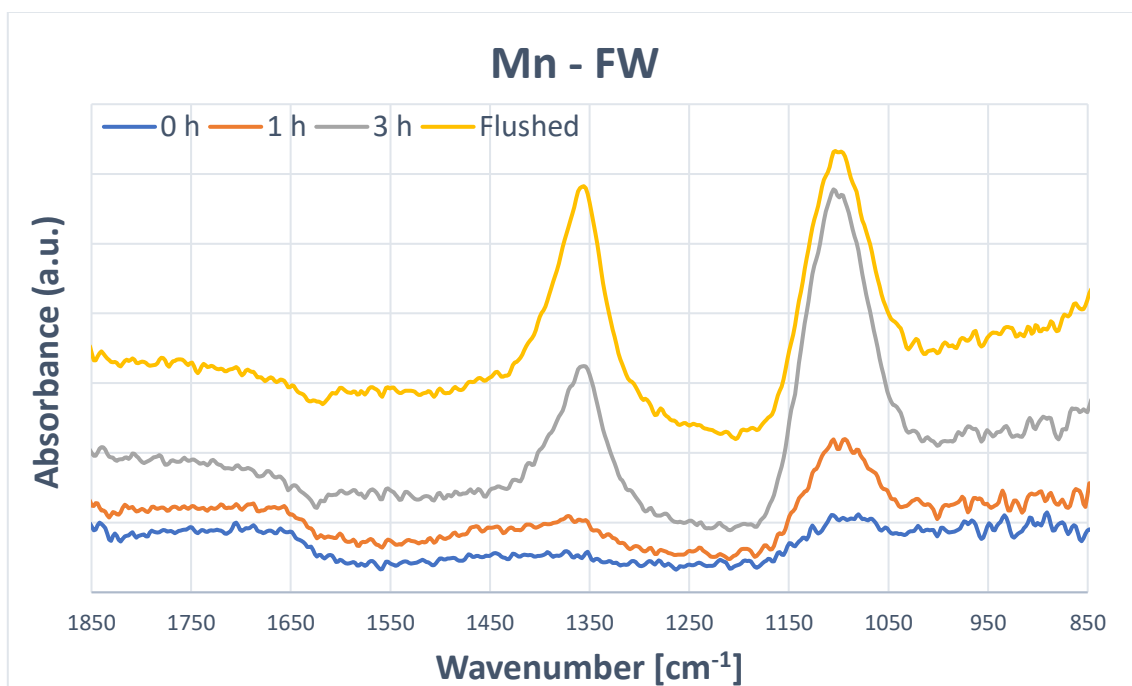
Figure 23. ATR-FTIR spectra of Mn NPs in FW. Peaks can be seen at 1100 and 1363 cm^{-1}.
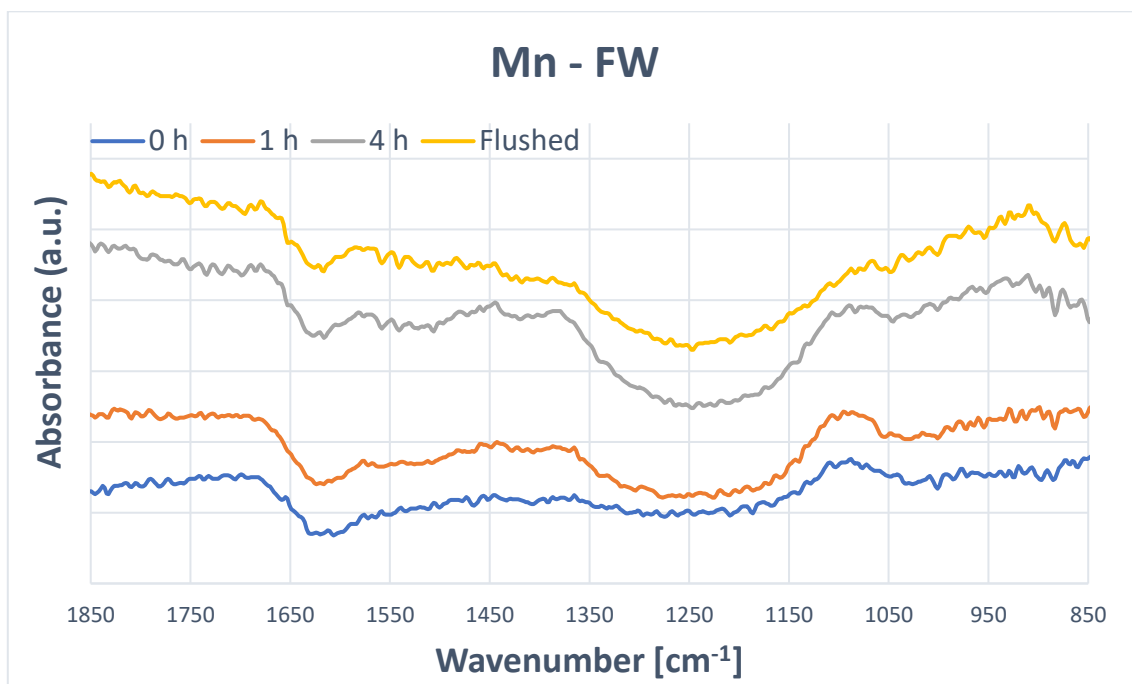
Figure 24. ATR-FTIR spectra of Mn NPs in FW. Peaks can be seen at 1100 and 1386 cm^{-1}.

Figure 25 and 26 shows the spectra for Mn_3O_4 NP films without NOM. These had peaks around 1089, 1157, 1385, and 1565 cm^{-1}.
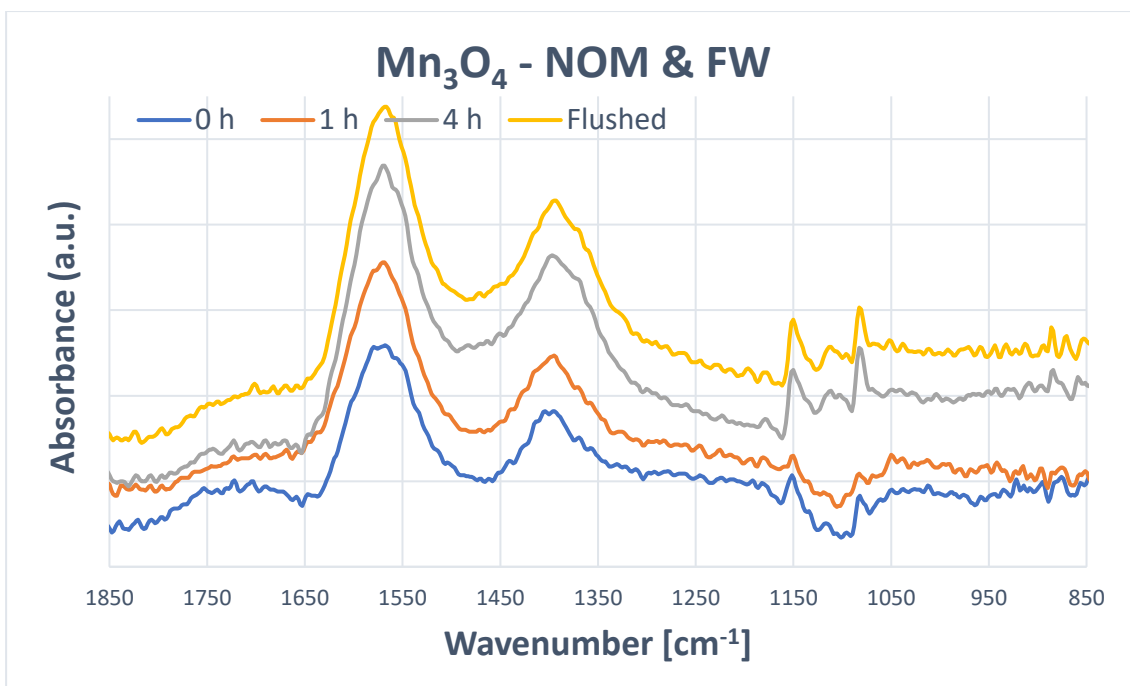
Figure 25. ATR-FTIR spectra of Mn₃O₄ NPs in FW and NOM. Peaks can be seen at 1083, 1160, 1400 and 1577 cm^{-1}.
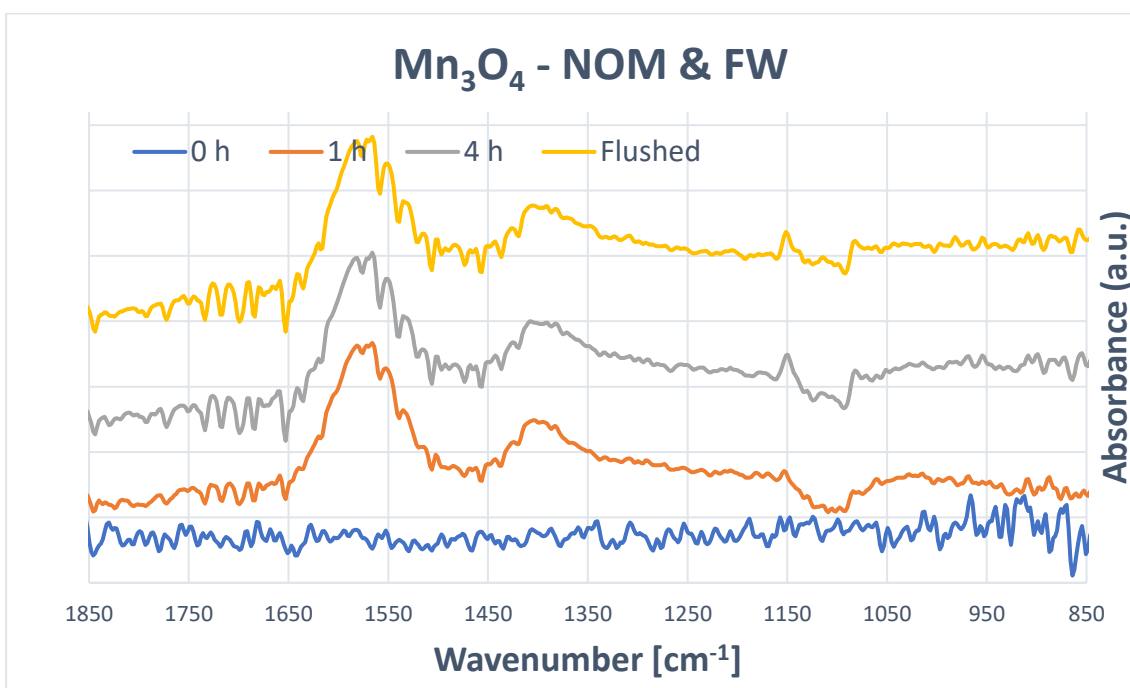
Figure 26. ATR-FTIR spectra of Mn₃O₄ NPs in FW and NOM. Peaks can be seen at 1085, 1155, 1405 and 1575 cm^{-1}.

In Figure 27 and 28 the spectra for Mn₃O₄ NP films without NOM are shown. These had peaks around 1100, 1385, 1454, and 1575 cm^{-1}.
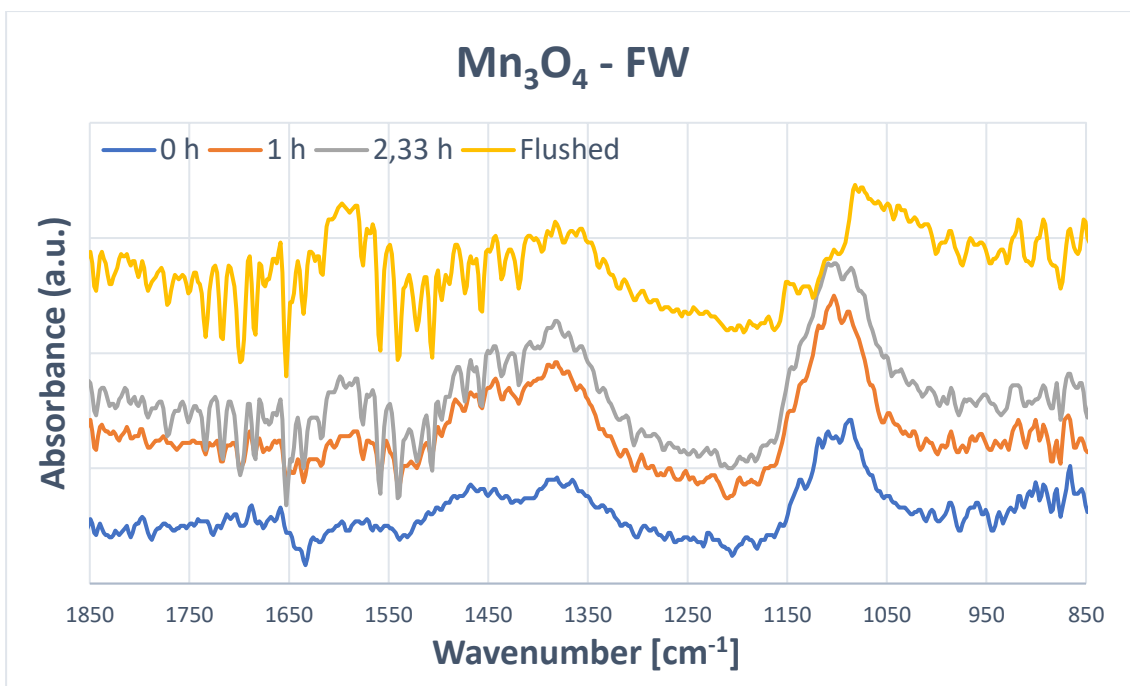
Figure 27. ATR-FTIR spectra of Mn₃O₄ NPs in FW. Peaks can be seen at 1100, 1386, 1454 and 1598 cm^{-1}.
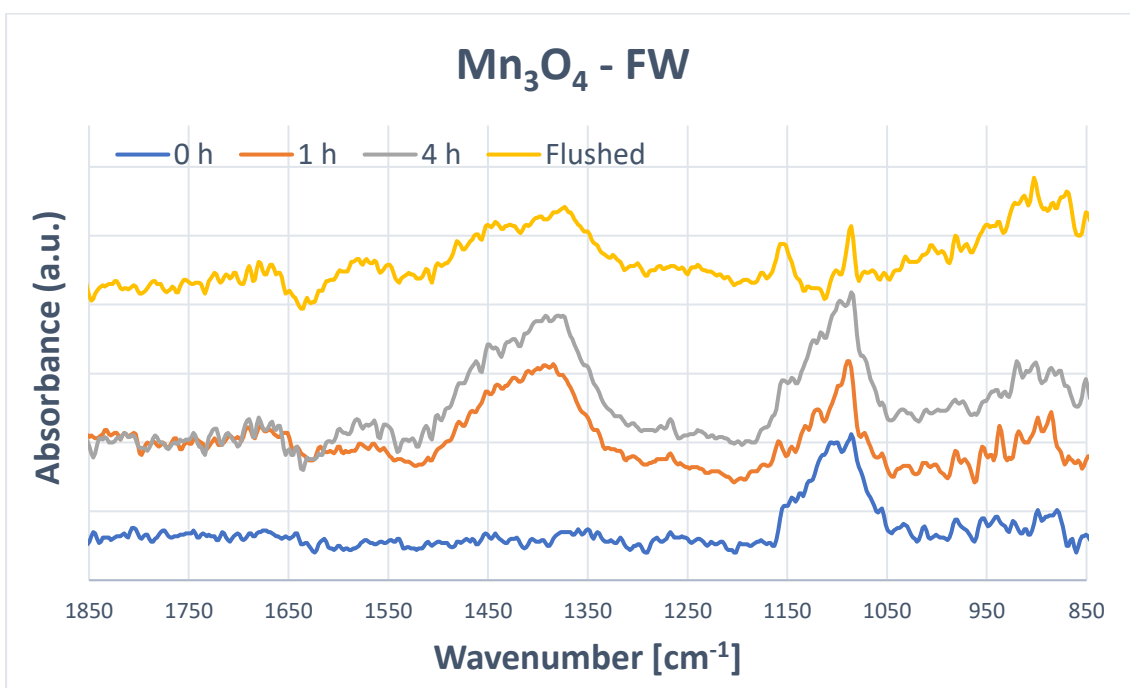
Figure 28. ATR-FTIR spectra of Mn₃O₄ NPs in FW. Peaks can be seen at 1095, 1384, and 1575 cm^{-1}.

A summary of the peaks identified from the different IR measurements is compiled in Table 6. Six different peak main peaks were noted when identifying the peak using OPUS. From Table 6 it is clear that the most common peaks across the measurements were approximately around 1100, 1385 and 1565 cm⁻¹ for the Mn and Mn₃O₄ NP films in solutions containing FW and NOM, and 1100 and 1385 cm⁻¹ in FW only. For the Mn NPs films in NOM

a peak around 1700 cm^{-1} was seen in addition, and for the Mn$_3$O$_4$ NPs in NOM an extra peak around 1160 cm^{-1} showed up. All the peaks were quite broad, except for peak 1-2 in Mn$_3$O$_4$-FW, but were centered around these numbers. This suggests that there could more than one peak which contributes to a broader peak.

Table 6. A compilation of all the obtained peaks corresponding to all the samples from ATR testing.

Test	Peak 1 [cm^{-1}]	Peak 2 [cm^{-1}]	Peak 3 [cm^{-1}]	Peak 4 [cm^{-1}]	Peak 5 [cm^{-1}]	Peak 6 [cm^{-1}][-1]
Mn-FW-1	1100	-	1363	-	-	-
Mn-FW-2	1100	-	1386	-	-	-
Mn-NOM-1	1100	-	1388	-	1575	1730
Mn-NOM-2	1100	-	1398	-	1577	1689
Mn$_3$O$_4$-FW-1	1100	-	1386	1454	1598	-
Mn$_3$O$_4$ - FW-2	1095	-	1384	-	1589	-
Mn$_3$O$_4$-NOM-1	1083	1160	1400	-	1577	-
Mn$_3$O$_4$-NOM-2	1085	1155	1405	-	1575	-

Some conclusions of what these peaks represent can be drawn from using literature values and the knowledge of the contents of the solutions. Since sulfate, SO_4^{2-}, and carbonate, CO_3^{2-}, are present in FW it is therefore likely that these will adsorb onto the particles as well. These appear as active absorption bands around 1100 cm^{-1} for sulfate [91] [92] [93]. Carbonate has a spectrum with absorption bands at approximately 1385–1390 cm^{-1} as a result of asymmetrical stretching [94] [95]. Peaks at 1065 cm^{-1} and 885 cm^{-1} are also present in the spectra as a result of symmetrical stretching of carbonate [94]. Therefor the peaks that are seen around 1100 cm^{-1} and 1380-1390 cm^{-1} are likely to be at least by some capacity caused by adsorption of carbonate and sulfate. For some of the sample, such as Mn NPs in FW and NOM and Mn NPs in FW, a small peak at around 885 cm^{-1} can also be noted but since the noise is quite high this is hard to confirm.

As mentioned before, carboxylate, COO$^-$ is largely present in NOM and its presence can be used to determine whenever NOM has adsorbed on to the NPs. In ATR-IR it showed up at 1380 cm^{-1} and 1575 cm^{-1} and caused by symmetrical stretching and asymmetrical stretching of COO$^-$, respectively [96]. In the NOM samples peaks within this range were found which correspond well to these numbers. Peak 1, at approximately 1100 cm^{-1}, may also have contribution from NOM components [14]. The peaks around 1690-1750

cm^{-1} might also stem from C=O bonds, which most likely is caused by protonated carboxylate groups [97].

5.4 Reactive oxygen species

Figures 29 and 30 show ROS activity using the DCFH method. The figures are the same except that Figure 30 includes the standard deviations from repeated experiments. Both graphs have been divided with their respective blanks (solutions without NPs), which enables the ROS activity to be directly comparable between the different NPs and solutions. There is no significant increase in ROS activity in the presence of NPs, as seen when the standard deviations are added.
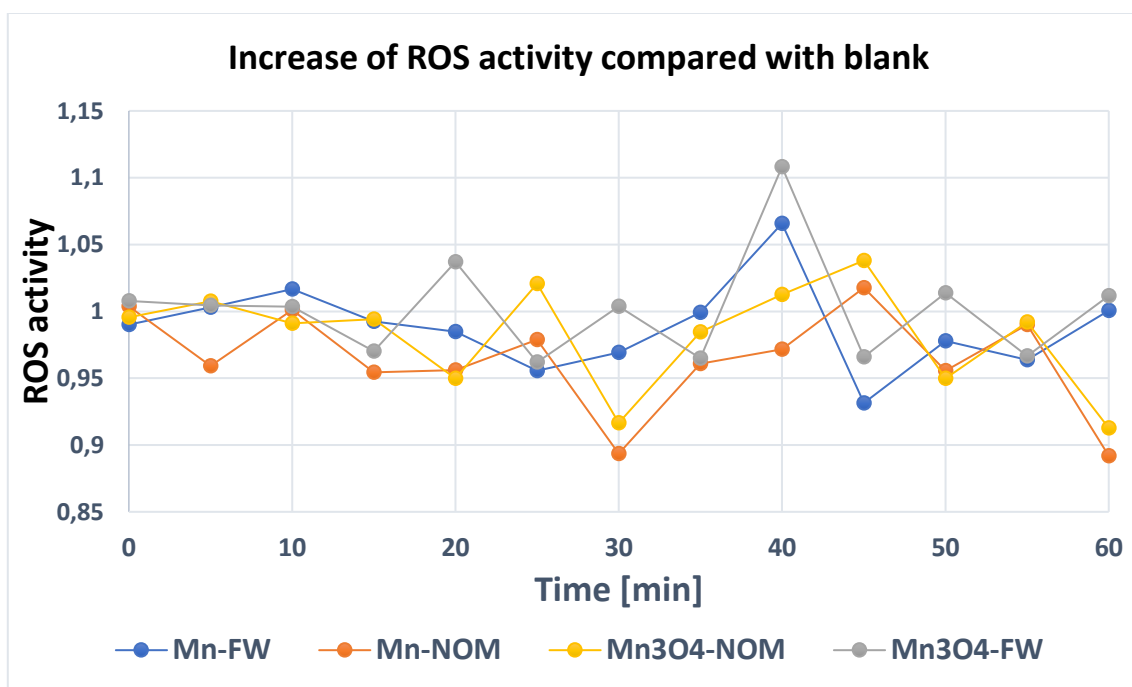
Figure 29. Changes in ROS activity over times. All the values have been divided with there respective blank sample.
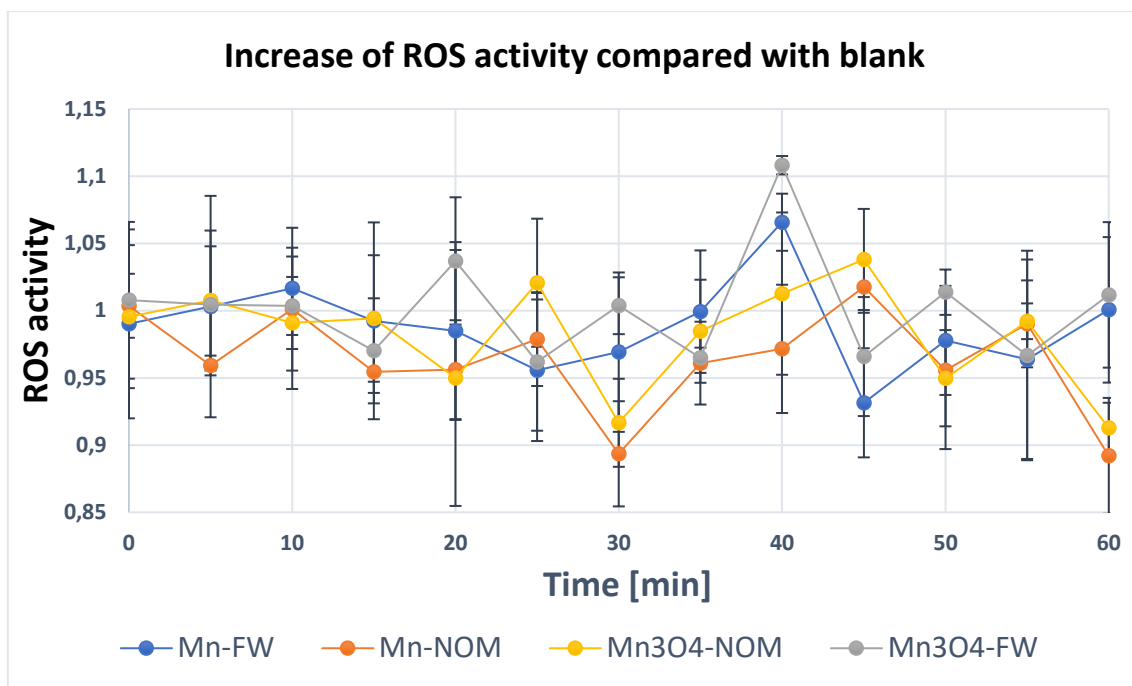
Figure 30. Changes in ROS activity over times. All the values have been divided with there respective blank sample. The error bars represent the standard deviations from four replicas.

5.5 Visual MINTEQ

Table 7 shows the results from Visual MINTEQ calculations. A decrease in Mn ion concentration decreases the percentage of free Mn ions as well increases the percentage Mn adsorbed to NOM. The amount of Mn with adsorbed NOM is 9.5-10.1%. There were close to no amount of Mn^{3+} in any of the simulation runs and it is therefore not included in the table.

Around 4.5% of the adsorbed NOM was bounded to the Mn electrostatically, which is a weaker form of binding. The other bonded NOM, ca 5.5 %, formed a monodentate complex with the Mn. Both of these were bounded in the dissolved phase.

Table 7. A summary of Visual MINTEQ results from metal speciation simulations of Mn^{2+} in FW with and without NOM.

	Covalently bound Mn-NOM	Weakly bound Mn-NOM	Mn^{2+}	$MnCl^+$	$MnSO_4$ (aq)	$MnHCO_3$
Mn 1 mg/L With NOM	5.3 %	4.3 %	89.8 %	0.04 %	0.6 %	0.05 %
Mn 0.4 mg/L With NOM	5.4 %	4.5 %	89.4 %	0.04 %	0.6 %	0.05 %
Mn 0.3 mg/L With NOM	5.4 %	4.5 %	89.4 %	0.04 %	0.6 %	0.05 %
Mn 0.25 mg/L With NOM	5.4 %	4.5 %	89.4 %	0.04 %	0.6 %	0.05 %
Mn 0.2 mg/L With NOM	5.5 %	4.5 %	89.3 %	0.04 %	0.6 %	0.05 %
Mn 0.05 mg/L With NOM	5.5 %	4.6 %	89.2 %	0.04 %	0.6 %	0.05 %
Mn 1 mg/L Without NOM	-	-	99.2 %	0.04 %	0.6 %	0.05 %
Mn 0.4 mg/L Without NOM	-	-	99.2 %	0.04 %	0.7 %	0.06 %
Mn 0.3 mg/L Without NOM	-	-	99.2 %	0.04 %	0.7 %	0.06 %
Mn 0.25 mg/L Without NOM	-	-	99.2 %	0.04 %	0.7 %	0.06 %
Mn 0.2 mg/L Without NOM	-	-	99.2 %	0.04 %	0.7 %	0.06 %
Mn 0.05 mg/L Without NOM	-	-	99.2 %	0.04 %	0.7 %	0.06 %

6. Discussion

6.1 Surface interactions and particle size

In the presence of NOM there is co-adsorption between NOM, and carbonate and sulfur (Table 6). It was also seen that the intensity of the different peaks went up when comparing short exposure, within the first 5 minutes, to later exposure, 2-4 h. This implies that the amount of NOM and other species at the surface are increasing over time and might even adsorb in multiple layers onto the NPs [98].

When comparing the Mn and Mn_3O_4 NPs some similarities and differences can be spotted. When the Mn film was left in FW only two peaks appeared. These corresponds to adsorption of sulfur and carbonate. However, the Mn_3O_4 NPs in the same solution showed two additional peaks, at approximately 1454 and 1593 cm^{-1}. Since NOM is not present here this indicates more configurations for carbonate which also can cause these peaks [99]. Since more than one confirmation is seen it is very possible that Mn_3O_4 NPs have a heterogeneous surface, meaning that there might be different binding sites where ligands can be adsorbed.

In the NOM solution the most apparent difference is that the Mn NPs showed peaks at around 1730 cm^{-1} which the Mn_3O_4 NPs did not. This peak most likely corresponds to protonated carboxylate groups origination from NOM. The reason as to why this peak is only seen for the Mn NPs might be that these particles have lower surface pH compared to the Mn_3O_4 NPs, but this cannot be confirmed. For the Mn_3O_4 NPs where was also two peaks in the 1080-1160 region and only one broader for the Mn NPs. But since the Mn NPs peak was quite broad here it might just be a combination of the two more narrow ones which were seen for the Mn_3O_4 NPs.

The peaks mostly stayed intact when rinsing the samples with ultrapure water after the first measurement of the adsorption using ATR-FTIR. This indicates that the adsorption is at least strong enough to not loosen due to that much mechanical strain. However, in order to figure out more precisely how strongly adsorbed the particles are some sort of quantification study would be necessary. An idea for such a study could be to add other ligands or molecules which have a high affinity towards the manganese and manganese oxide NPs to see if they overtime will replace NOM.

When using Visual MINTEQ it was found that Mn ions (Mn^{2+}) had a much higher affinity towards NOM compared with sulfate and carbonate (see Table 6). Due to this, it is likely that a lot of the peaks in the area where carboxylate can be seen probably is heavily contributed by NOM. Two types of binding were seen between NOM and Mn: one weak electrostatic and one monodentate, covalent complex. Since the complex is monodentate this means that only one atom in in each of the ligands are bound to the metal atom [100].

6.2 Dissolution

6.2.1 Problem with repeatability for dissolution tests of Mn_3O_4 NPs

The dissolution data for Mn_3O_4 NPs showed varying results for different batches. In batch 1 and 2 the concentration of Mn decreased over time, while in batch 3 and 4 this was not the case. Since the results are quite contradictory when compared to each other it is likely that at least some, or all of them, either have been prepared poorly or that another error source, for example contamination, has occurred.

The varying results between the batches may be caused by a few different things. One of them being contamination. For three samples, B1-Mn_3O_4-FW+NOM-24h, B3-Mn_3O_4-FW-1h and B3-Mn_3O_4-FW+NOM-2h, the blanks showed quite high amount of Mn. This indicates that some contamination possibly occurred for some of the samples. The source of this might be contaminations from a previous step, such as that some NPs may have entered the samples when removing the supernatant after centrifugation. This can happen if the samples get stirred too much or if the pipet pokes at the bottom of the sample when extracting the supernatant. Another reason could be that the particles were not separated properly during centrifugation. However, to test this, a few NTA analyses was performed on the ultracentrifuged supernatant for samples with and without NOM, and almost no particles were found during this. Also, when viewing previous work regarding similar NPs, centrifugation seems to work fine, which indicates that this should not be the problem [101]. The most likely reason for this variation is probably that the number of particles extracted from the sonicated stock solution was not repeatable across the different batches and samples. This can happen if the samples are not sonicated long enough or if the particles sediment very quickly after sonication. This is further supported viewing figure 10-11 since the values varied quite a bit.

However, a different preparation method might need to be used in order to minimize interference with the results. It is hard to know to what extent the samples were affected by the dispersion preparation and exactly the cause of the variation in results between batches, but fast sedimentation of the NPs and/or some type of contamination seems like plausible sources of error. Maybe the preparation can be modified to create a more stable dispersion by changing the method by employing a more frequent sonification of the stock solution and the intermediate solution in step 2. If these solutions are mixed more frequently the NPs can be extracted from them approximately at the same time every time after sonication every, which might reduce the effect of sedimentation since if any sedimentation is occurring it would have similar effects on all samples then. Another suggestion would be to add a chemical which would hinder agglomeration of the particles thus making it a more stable suspension. However, since this chemical should not interfere with the mechanisms of NOM it would be hard to find such a chemical.

Some inconsistencies between the data can be noted when viewing the tests which are divided with their respective total concentration tests. For manganese NPs, the dissolution percentage is quite high, as seen in Figure 7. For one sample, Mn-NOM-6 h the dissolution is over 100% which should be impossible. One possible explanation for this is that the sedimentation of the particles in the stock solution was quicker than anticipated. Since the

stock solution was first added to the respective samples 1-3 and afterwards added to the total concentration test there was some delay between the additions. If the stock solution sedimented fast this may have led to different amounts of Mn depending on at which time the stock solution was added. For the manganese oxide NP samples which were prepared after the manganese NP tests, the solution was more frequently mixed and shaken between pipetting into the samples.

6.2.2 Dissolution of Mn and Mn_3O_4 NPs

Regardless of the uncertainties, some interpretations of the dissolution data till be made in this section. In Figure 6 the dissolution in FW for the manganese NPs was somewhat higher than in FW with NOM for all the exposure times. This gap also seems to become especially large for the 24 H exposure where this difference also becomes statistically significant. This indicates that the dissolution in the solution which contains NOM may be slightly inhibited compared to the one which only contains FW. Since the addition of NOM is the only difference between the two this inhibition is most likely caused by adsorbed NOM (detected by ATR-FTIR).

When analyzing the data from the NTA very large standard deviation values were received. Since these values in most cases were larger than the measured values themselves the data is not trustworthy. The reason for this is probably due to the low concentration of particles which was used, in addition to sedimentation. Since the samples used in NTA retrieved from the samples which were prepared for AAS the concentration of these were very low in order to mimic real conditions in nature. However, due to this low concentration there were two few particles present for the NTA to give a fair analysis. Since the NTA analyses particles from a few different parts of the sample there needs to be enough particles throughout the sample so that these parts can be homogeneous and comparable. Otherwise, which probably were the case here, the different parts of the sample which are analyzed will be very different from each other and therefor yield high errors when compared. Therefore, if this were to be redone a separate sample with a more suitable concentration should be prepared. However, even if the concentration is hard to determine the sizes of the particles and agglomerates found are still valid and can provide information. The sizes found when investigating Mn_3O_4 NPs did not notably differ depending on if the solution contained NOM or, which indicates that NOM does not change size of the Mn_3O_4 agglomerates. For the Mn NPs a bit more larger particles were seen when NOM was present but since this difference was not significant, no conclusions can be drawn.

When viewing the concentration data from the NTA, the suspensions which contained NOM seemed to have higher amounts of bigger particles compared to the FW solution, as seen from the NTA analysis. This further supports that the NOM solution might slow down dissolution of the particles. If dissolution were occurring at the same rate for all the samples not a lot of difference would be seen when NOM was present, however since a small difference can be noted this indicates a decrease in dissolution rate.

Since Visual MINTEQ is a rather simple model it can only give a rough idea as to what will happen in such a system under simplified conditions. Some assumptions which are made are for example that only fulvic acids, not humic acids, may be dissolved. This means that all

the active NOM is only fulvic acids. Since NOM-Mn interactions in this simulation only occurred in the dissolved phase, only interactions with fulvic acids have been considered. In reality, NOM is made up of a lot of humic acids as well. However, since humic acids are considered to be in insoluble in water at acidic pH and the pH used in this study, 6.2, is slightly acidic, this assumption probably will not affect the reliability of the results too much [102]. Other assumptions made are the shape of the fulvic and humic acids. Dissolved fulvic acids are assumed to be spheres while the solid fulvic and humic acids are assumed to have a planar geometry. These of course a simplification of the problem since the shapes of both in reality are much more diverse. Despite this a rather good approximation can be made using the software [83].

6.3 Generation of reactive oxygen species

As seen in figure 35 and 36, there was no apparent sign of increasing ROS when adding NPs to FW and FW with NOM solution. However, the method used can only detect certain types of ROS while others, for example hydrogen peroxide, cannot be detect by the method. This means that there might still be an increase in ROS activity even if it was not shown by these tests. Since release of ions as a result of electrochemistry is known to sometimes generate ROS, it is not unlikely that H_2O_2 might have been produced [103]. Especially since moderate ion release was confirmed by AAS analysis, as well as in other works [104].

It is also possible that the adsorbed ligands, which were confirmed in the ATR-FTIR analysis, might block reactions needed for ROS generation and therefor reduce the ROS generation as a total.

Therefore, it would be of interest to perform more ROS tests to find out if there is any increase in ROS activity by any kind of ROS. However, since Mn NPs has shown to cause an increase of hydrogen peroxide at least in some biological media, it would be very interesting to test if this in the case even in the FW and/or NOM solution as well [105].

7. Conclusions

There is most likely a need to revise the methods for the sample preparation both for AAS and NTA measurements. For AAS more consistent mixing is needed when pipetting in order to combat problems with fast sedimentation and agglomeration. For NTA measurements, separately prepared samples with a more suitable concentration would likely result in more reliable results.

The AAS and NTA results which were received point towards a slower dissolution when NOM is present for both the NPs. This is seen by a generally lower concentration of Mn in the samples where NOM was added in the AAS experiments and by a generally higher number of larger particles when NOM was added in NTA.

From the ATR-IR measurements adsorption of sulfur, carbonate, and NOM, if present, could be confirmed for both Mn and Mn_3O_4 NPs. Due to the increasing intensity of the peaks over time the adsorption might happen in more than one layer onto the NPs.

No sign of increasing ROS activity was found when using a DCHF method. However, this did not test for increased hydrogen peroxide activity which might still be present.

From simulations Visual MINTEQ simulations it was found that approximately 10 % of Mn ions were attached to NOM w when using a Mn ion concentration of 0.05-1 mg/L Mn. Of these 10 % around 4.5% was weakly adsorbed electrostatically white the other 5.5 % formed a monodentate complex with NOM.

8. Future work

There is a lot which can be done in this area which could not be fitted into this report. Therefore, the focus of this section is on complimentary studies to help better understand the properties, persistence and toxicity of Mn and Mn_3O_4.

A study which investigates the size distribution on NP samples which has been exposed to NOM would be interesting. This could be a study with NTA which has a more appropriate concentration for NTA or maybe a DLS study.

Since ROS such as H_2O_2 could not be investigated in this study it would be of interest to do similar ROS tests where changes of this kind of ROS may be detected. Doing zeta potential studies would also be interesting to further study the particles agglomeration tendencies.

Other interesting studies would be on the type of binding which occurs between the NPs and NOM. For example, by adding phosphate ions to see is it influences the adsorption. If it is only ligand exchange which is occurring this should have a large effect. If it does not, then there are likely to be other adsorption mechanisms than ligand adsorption present [106] [107].

9. Acknowledgements

To start of I would like to express gratitude to my supervisor Jonas Hedberg, doctor at KTH Royal Institute of Technology, for the endless support and patience which he has given throughout this project. Without his valuable advice and ideas this project would not be what is today. I would also wholeheartedly like to thank professor Inger Odnevall Wallinder, associate professor Eva Blomberg and Amanda Kessler, all employees at KTH Royal Institute of Technology, for the kind and valuable advice and guidance which they have provided throughout this project.

With this being my final work before graduation I would also like thank the inspiring and wonderful friends that have been by my side these last 5 years, without your endless support this journey which I have had the privilege of making would not have been possible. A special thanks to Alexander Wärnheim, Bianca Otake, Josefin Svenson, Line Larby and Souzan Hammadi, all students or former students at Materials design, for making this these years so fun and meaningful!

10. References

[1]   M. F. Hochella, D. W. Mogk, J. Ranville, I. C. Allen, G. W. Luther, L. C. Marr, P. McGrail, M. Murayama, N. P. Qafoku, K. M. Rosso, N. Sahai, P. A. Schroeder, P. Vikesland, P. Westerhoff och Y. Yang, "Natural, incidental, and engineered nanomaterials and their impacts on the Earth system," *Science,* vol. 363, nr 6434, 2019.

[2]   M. E. K. T. V. E. P. M. S. P. H. J. M. F. R. D. a. H. M. S. Vance, "Nanotechnology in the real world: Redeveloping the nanomaterial consumer products inventory," *Beilstein J. Nanotechnologi,* nr 6, pp. 1769-1780, 2015.

[3]   S. F. H. L. R. B. P. R. M. A. B. A. a. B. A. Hansen, "Nanoproducts – what is actually available to European consumers?," *Environmental Science: Nano,* nr 3, pp. 169-180, 2016.

[4]   G. V. Lowry, K. B. Gregory, S. C. Apte och J. R. Lead, "Transformations of Nanomaterials in the Environment," *Environmental Science & Technology,* vol. 46, nr 13, pp. 6893-6899, 2012.

[5]   S. F. S. S. N. S. L. M. H. N. B. a. B. A. Hansen, "Revising REACH guidance on information requirements and chemical safety assessment for engineered nanomaterials for aquatic ecotoxicity endpoints: recommendations from the EnvNano project.," *Environmental Sciences Europe volume,* vol. 29, nr 14, 2017.

[6]   L. R. Pokhrel, B. Dubey och P. R. Scheuerman, "Natural water chemistry (dissolved organic carbon, pH, and hardness) modulates colloidal stability, dissolution, and antimicrobial activity of citrate functionalized silver nanoparticles," *Environmental Science: Nano,* nr 1, pp. 45-54, 2014.

[7]   P. Luo, I. Morrison, A. Dudkiewicz, K. Tiede, E. Boyes, P. O'toole, S. Park och A. Boxall, "Visualization and characterization of engineered nanoparticles in complex environmental and food matrices using atmospheric scanning electron microscopy," *Journal of microscopy,* vol. 250, nr 1, pp. 32-41, 2013.

[8]   R. E. Özel, K. N. Wallace och S. Andreescu, "Alterations of intestinal serotonin following nanoparticle exposure in embryonic zebrafish," *Environmental Science: Nano,* nr 1, pp. 27-36, 2014.

[9]   M. Auffan, J. Rose, J.-Y. Bottero, G. V. Lowry, J.-P. Jolivet och M. R. Wiesner, "Towards a definition of inorganic nanoparticles from an environmental, health and safety perspective," *Nature Nanotechnology,* vol. 4, p. 634–641, 2009.

[10]   M. F. Hochella, S. K. Lower, P. A. Maurice, R. L. Penn, N. Sahai, D. L. Sparks och B. S. Twining, "Nanominerals, Mineral Nanoparticles, and Earth Systems," *Science,* vol. 319, nr 5870, pp. 1631-1635, 2008.

[11]   M. Haruta, "Gold as a novel catalyst in the 21st century: Preparation, working mechanism and applications.," *Gold Bulletin,* nr 37, p. 27–36, 2004.

[12] T. R. H. R. J. a. P. J. A. Kuech, "Chemical transformation of metal, metal oxide, and metal chalcogenide nanoparticles in the environment," i *Engineered Nanoparticles and the Environment: Biophysicochemical Processes and Toxicity*, John Wiley & Sons, 2016, pp. 261-343.

[13] A. Nel, T. Xia, L. Mädler och N. Li, "Toxic Potential of Materials at the Nanolevel," *Science,* vol. 311, nr 5761, pp. 622-627, 2006.

[14] I. A. Mudunkotuwa och V. H. Grassian, "Biological and environmental media control oxide nanoparticle surface composition: the roles of biological components (proteins and amino acids), inorganic oxyanions and humic acid," *Environmental Science: Nano,* vol. 2, nr 5, pp. 429-439, 2015.

[15] A. R. Petosa, D. P. Jaisi, I. R. Quevedo, M. Elimelech och N. Tufenkji, "Aggregation and Deposition of Engineered Nanomaterials in Aquatic Environments: Role of Physicochemical Interactions," *Environmental Science & Technology,* vol. 44, nr 17, pp. 6532-6549, 2010.

[16] C. Levard, B. C. Reinsch, F. M. Michel, C. Oumahi, G. V. Lowry och G. E. Brown, "Sulfidation Processes of PVP-Coated Silver Nanoparticles in Aqueous Solution: Impact on Dissolution Rate," *Environmental Science & Technology,* vol. 45, nr 12, pp. 5260-5266, 2011.

[17] S. Diegoli, A. L. Manciulea, S. Begum, I. P. Jones, J. R. Lead och J. A. Preece, "Interaction between manufactured gold nanoparticles and naturally occurring organic macromolecules," *Science of The Total Environment,* vol. 402, nr 1, pp. 51-61, 2008.

[18] J. Fabrega, S. R. Fawcett, J. C. Renshaw och J. R. Lead, "Silver Nanoparticle Impact on Bacterial Growth: Effect of pH, Concentration, and Organic Matter," *Environmental Science & Technology,* vol. 43, nr 19, pp. 7285-7290, 2009.

[19] D. Li, D. Y. Lyon, Q. Li och P. J. J. Alvarez, "Effect of soil sorption and aquatic natural organic matter on the antibacterial activity of a fullerene water suspension," *Environmental Toxicology and Chemistry,* vol. 27, nr 9, pp. 1888-1894, 2008.

[20] FN, "Regeringen.se," Sveriges Regering, 14 December 2015. [Online]. Available: https://www.regeringen.se/regeringens-politik/globala-malen-och-agenda-2030/ekosystem-och-biologisk-mangfald/. [Använd 13 November 2020].

[21] FN, "Regeringen.se," Sveriges regering, 3 December 2015. [Online]. Available: https://www.regeringen.se/regeringens-politik/globala-malen-och-agenda-2030/hallbar-industri-innovationer-och-infrastruktur/. [Använd 13 November 2020].

[22] R. N. Reddy och R. G. Reddy, "Synthesis and electrochemical characterization of amorphous MnO2 electrochemical capacitor electrode material," *Journal of Power Sources,* vol. 132, nr 1-2, pp. 315-320, 2004.

[23] Y. Chen, C. Liu, F. Li och H.-M. Cheng, "Preparation of single-crystal α-MnO2 nanorods and nanoneedles from aqueous solution," *Journal of Alloys and Compounds,* vol. 397, nr 1-2, pp. 282-285, 2005.

[24] P. Z. Si och D. Li, "Unconventional exchange bias in oxide-coated manganese nanoparticles,"

Applied Physics Letters, vol. 87, nr 133122, 2005.

[25] S. Zhu, S.-H. Ho, C. Jin, X. Duan och S. Wang, "Nanostructured manganese oxides: natural/artificial formation and their induced catalysis for wastewater remediation," *Environmental Science: Nano,* vol. 7, nr 2, pp. 368-396, 2020.

[26] C. Felton, A. Karmakar, Y. Gartia, P. Ramidi, A. S. Biris och A. Ghosh, "Magnetic nanoparticles as contrast agents in biomedical imaging: recent advances in iron- and manganese-based magnetic nanoparticles," *Drug Metabolism Reviews ,* vol. 46, nr 2, pp. 142-154 , 2014.

[27] J. Zhao och M. Riediker, "Detecting the oxidative reactivity of nanoparticles: a new protocol for reducing artifacts," *Journal of Nanoparticle Research,* vol. 16, nr 2493, 2014.

[28] X. Xie, Z. He, N. Chen, Z. Tang, Q. Wang och Y. Cai, "The Roles of Environmental Factors in Regulation of Oxidative Stress in Plant," *Biomed Res International,* 2019.

[29] V. Stone, J. Shaw, D. Brown, W. MacNee, S. Faux och K. Donaldson, "The role of oxidative stress in the prolonged inhibitory effect of ultrafine carbon black on epithelial cell function," *Toxicology in Vitro,* vol. 12, nr 6, pp. 649-659, 1998.

[30] M. R. Wilson, J. H. Lightbody, K. Donaldson, J. Sales och V. Stone, "Interactions between Ultrafine Particles and Transition Metals in Vivo and in Vitro," *Toxicology and Applied Pharmacology,* vol. 184, nr 3, pp. 172-179, 2002.

[31] E. Koike och T. Kobayashi, "Chemical and biological oxidative effects of carbon black nanoparticles," *Chemosphere,* vol. 65, nr 6, pp. 946-951, 2006.

[32] S. McCarrick, F. Cappellini, A. Kessler, N. Moelijker, R. Derr, J. Hedberg, S. Wold, E. Blomberg, I. Odnevall Wallinder och G. Hendriks, "oxTracker Reporter Cell Lines as a Tool for Mechanism-Based (Geno)Toxicity Screening of Nanoparticles—Metals, Oxides and Quantum Dots," *Nanomaterials ,* vol. 110, nr 10, 2020.

[33] V. P. S. S. M. M. M. L. a. K. A. Aruoja, "Toxicity of 12 metal-based nanoparticles to algae, bacteria and protozoa," *Environmental Science: Nano,* nr 2, pp. 630-644, 2015.

[34] R. Grillo, A. H. Rosa och L. F. Fraceto, "Engineered nanoparticles and organic matter: A review of the state-of-the-art," *Chemosphere,* vol. 119, pp. 608-619, 2015.

[35] Mistra, "Mistra," [Online]. Available: https://www.mistra.org/en/research/mistra-environmental-nanosafety/. [Använd 2 06 2020].

[36] S. Bhattacharjee, "DLS and zeta potential – What they are and what they are not?," *Journal of Controlled Release,* vol. 235, pp. 337-351, 2016.

[37] Y. S. P. S. C. F. K. M.-E. B. E. K. H. O. W. I. a. H. J. F. Hedberg, "Electrochemical surface oxide characteristics of metal nanoparticles (Mn, Cu and Al) and the relation to toxicity," *Electrochimica Acta,* vol. 212, pp. 360-371, 2016.

[38] Y. S. P. S. C. F. K. M.-E. B. E. K. H. O. W. I. a. H. J. F. Hedberg, "Electrochemical surface oxide characteristics of metal nanoparticles (Mn, Cu and Al) and the relation to toxicity,"

Electrochimica Acta, vol. 212, pp. 360-371, 2016.

[39] G. Sposito, The Chemistry of Soils, Oxford: Oxford University Press, 1989.

[40] F. J. Stevenson, Humus Chemistry: Genesis, Composition, Reactions., New York: John Wiley and Sons, 1994.

[41] M. B. Hay och S. C. Myneni, "Structural environments of carboxyl groups in natural organic molecules from terrestrial systems. Part 1: Infrared spectroscopy," *Geochimica et Cosmochimica Acta,* vol. 71, p. 3518–3532, 2007.

[42] G. J. D. S. och J. E. Scott, " Infrared frequency and dissociation constant of the carboxylate group.," *Nature,* nr 220, p. 698–699, 1968.

[43] S. Cabaniss, J. Leenheer och I. McVey, "Aqueous infrared carboxylate absorbances: aliphatic di-acids," *Spectrochimica Acta Part A: Molecular and Biomolecular Spectroscopy,* vol. 53, nr 3, pp. 449-458, 1998.

[44] S. E. Cabaniss och I. F. McVey, "Aqueous infrared carboxylate absorbances: aliphatic monocarboxylates," *Spectrochimica Acta Part A: Molecular and Biomolecular Spectroscopy,* vol. 51, nr 13, pp. 2385-2395, 1995.

[45] M. Schnitzer och S. I. M. Skinner, "Organo-metallic interactions in soils: 4. Carboxyl and hydroxyl groups inorganic matter and metal retention.," *Soil Science,* vol. 99, nr 4, pp. 278-284, 1965.

[46] D. S. Gamble, M. Schnitzer och I. Hoffman, "Cu2+ – fulvic acid chelation equilibrium in 0.1 m KCl at 25.0 °C," *Canadian Journal of Chemistry,* vol. 48, nr 20, pp. 3197-3204, 1970.

[47] I. A. Mudunkotuwa, A. A. Minshid och V. H. Grassian, "ATR-FTIR spectroscopy as a tool to probe surface adsorption on nanoparticles at the liquid–solid interface in environmentally and biologically relevant media," *Analyst,* vol. 139, nr 5, pp. 870-881, 2014.

[48] J. Borcherding, J. Baltrusaitis, H. Chen, L. Stebounova, C.-M. Wu, G. Rubasinghege, I. A. Mudunkotuwa, J. C. Caraballo, J. Zabner, V. H. Grassian och A. P. Comellas, "Iron oxide nanoparticles induce Pseudomonas aeruginosa growth, induce biofilm formation, and inhibit antimicrobial peptide function," *Environmental Science: Nano,* nr 1, pp. 123-132, 2014.

[49] C.-N. Lok, C.-M. Ho, R. Chen, Q.-Y. He, W.-Y. Yu, H. Sun, P. K.-H. Tam, J.-F. Chiu och C.-M. Che, "Silver nanoparticles: partial oxidation and antibacterial activities," *JBIC Journal of Biological Inorganic Chemistry,* nr 12, 2007.

[50] J. Greeley och J. Nørskov, "Electrochemical dissolution of surface alloys in acids: Thermodynamic trends from first-principles calculations," *Electrochimica Acta,* vol. 52, nr 19, pp. 5829-5836, 2007.

[51] S. Bakardjieva, P. Bezdicïka och T. Grygar, "Reductive dissolution of microparticulate manganese oxides," *J Solid State Electrochem,* nr 4, pp. 306-313 , 1999.

[52] C. H. E. M. L. G. V. a. B. G. E. Levard, "Environmental Transformations of Silver Nanoparticles: Impact on Stability and Toxicity," *Environmental Science & Technology,* vol. 46, nr 13, pp. 6900-

6914, 2012.

[53] J. H. Duffus, ""Heavy metals" a meaningless term? (IUPAC Technical Report)," *Pure and Applied Chemistry,* vol. 74, nr 5, pp. 793-807, 2009.

[54] B. C. Reinsch, C. Levard, Z. Li, R. Ma, A. Wise, K. B. Gregory, G. E. J. Brown och G. V. Lowry, "Sulfidation of Silver Nanoparticles Decreases Escherichia coli Growth Inhibition," *Environmental Science & Technology,* vol. 46, nr 13, pp. 6992-7000, 2012.

[55] R. Ma, C. Levard, S. M. Marinakos, Y. Cheng, J. Liu, F. M. Michel, J. G. E. Brown och G. V. Lowry, "Size-Controlled Dissolution of Organic-Coated Silver Nanoparticles," *Environmental Science & Technology,* vol. 46, nr 2, pp. 752-759, 2012.

[56] P. Tanapon, S. Navid, S. Kevin, T. Robert D. och L. Gregory V., "Aggregation and Sedimentation of Aqueous Nanoscale Zerovalent Iron Dispersions," *Environmental Science & Technology,* vol. 42, nr 1, pp. 284-290, 2007.

[57] H. Ernest M., P. Tanapon och L. Gregory V., "Nanoparticle Aggregation: Challenges to Understanding Transport and Reactivity in the Environment," *Journal of Enviromental Quality,* vol. 39, nr 6, pp. 1909-1924, 2010.

[58] H. Ernest M., B. Jean-Yves och W. Mark R., "Theoretical Framework for Nanoparticle Reactivity as a Function of Aggregation State," *Langmuir,* vol. 26, nr 13, pp. 11170-11175, 2010.

[59] I. D. K. L. J. a. V.-J. E. Lynch, "Macromolecular Coronas and Their Importance in Nanotoxicology and Nanoecotoxicology," i *Frontiers of Nanoscience*, Amsterdam, Elsevier, 2014, pp. 127-156.

[60] B. P. G. Charron, C. Pfeiffer, Y. Zhao, J. M. de la Fuente, X. Liang, W. J. Parak och P. del Pino, "Interfacing Engineered Nanoparticles with Biological Systems: Anticipating Adverse Nano–Bio Interactions," *Small,* vol. 9, nr 9-10, pp. 1573-1584, 2012.

[61] D.-H. Tsai, M. Davila-Morris, F. W. DelRio, S. Guha, M. R. Zachariah och V. A. Hackley, "Quantitative Determination of Competitive Molecular Adsorption on Gold Nanoparticles Using Attenuated Total Reflectance–Fourier Transform Infrared Spectroscopy," *Langmuir,* vol. 27, nr 15, pp. 9302-9313, 2011.

[62] H. G. Bagaria, E. T. Ada, M. Shamsuzzoha, D. E. Nikles och D. T. Johnson, "Understanding Mercapto Ligand Exchange on the Surface of FePt Nanoparticles," *Langmuir,* vol. 22, nr 18, pp. 7732-7737, 2006.

[63] M. Baalousha, A. Manciulea, S. Cumberland, K. Kendall och J. R. Lead, "Aggregation and surface properties of iron oxide nanoparticles: Influence of ph and natural organic matter," *Environmental Toxicology and Chemistry,* vol. 27, nr 9, pp. 1875-1882, 2008.

[64] B. Collin, E. Oostveen, O. V. Tsyusko och J. M. Unrine, "Influence of Natural Organic Matter and Surface Charge on the Toxicity and Bioaccumulation of Functionalized Ceria Nanoparticles in Caenorhabditis elegans," *Environmental Science & Technology,* vol. 48, nr 2, pp. 1280-1289, 2013.

[65] G. R. Aiken, H. Hsu-Kim och J. N. Ryan, "Influence of Dissolved Organic Matter on the Environmental Fate of Metals, Nanoparticles, and Colloids," *Environmental Science &*

Technology, vol. 45, nr 8, pp. 3196-3201, 2011.

[66] Z. Z. L. Z. J. a. X. B. Wang, "Environmental processes and toxicity of metallic nanoparticles in aquatic systems as affected by natural organic matter†," *Environmental Science: Nano,* vol. 3, nr 2, pp. 240-255, 2016.

[67] A. T. Stone och H.-J. Ulrich, "Kinetics and reaction stoichiometry in the reductive dissolution of manganese(IV) dioxide and co(III) oxide by hydroquinone," *Journal of Colloid and Interface Science,* vol. 132, nr 2, pp. 509-522, 1989.

[68] S. Allard, U. Gunten, E. Sahli, R. Nicolau och H. Gallard, "Oxidation of iodide and iodine on birnessite (δ-MnO2) in the pH range 4–8," *Water Research,* vol. 43, nr 14, pp. 3417-3426, 2009.

[69] S. Allard, L. Gutierrez, C. Fontain, J.-P. Croué och H. Gallarda, "Organic matter interactions with natural manganese oxide and synthetic birnessite," *Science of The Total Environment,* vol. 583, pp. 487-495, 2017.

[70] S.Bernard, Ph.Chazal och M.Mazet, "Removal of organic compounds by adsorption on pyrolusite (β-MnO2)," *Water Research,* vol. 31, nr 5, pp. 1216-1222, 1997.

[71] Steve J.Hill; Andy S.Fisher, "Atomic Absorption, Methods and Instrumentation," i *Encyclopedia of Spectroscopy and Spectrometry (Third Edition)*, Elsevier, 2017, pp. 37-43.

[72] P. S. K. H. C. e. a. Hole, "Interlaboratory comparison of size measurements on nanoparticles using nanoparticle tracking analysis (NTA)," *Journal of Nanoparticle Research,* vol. 15, nr 2101, 2013.

[73] P. Hole, K. Sillence och P. Wick, "Interlaboratory comparison of size measurements on nanoparticles using nanoparticle tracking analysis (NTA)," *Journal of Nanoparticle Research,* vol. 15, nr 2101, 2013.

[74] V. Filipe, A. Hawe och W. Jiskoot, "Critical Evaluation of Nanoparticle Tracking Analysis (NTA) by NanoSight for the Measurement of Nanoparticles and Protein Aggregates," *Pharmaceutical Research,* vol. 27, p. 796–810, 2010.

[75] J. D. Schuttlefield och V. H. Grassian, "ATR–FTIR Spectroscopy in the Undergraduate Chemistry Laboratory. Part I: Fundamentals and Examples," *Journal of Chemical Education,* vol. 85, nr 2, p. 279, 2008.

[76] Thermo Fisher Scientific , "Thermo Fisher Scientific," Thermo Fisher Scientific Logo, [Online]. Available: https://www.thermofisher.com/se/en/home/industrial/spectroscopy-elemental-isotope-analysis/spectroscopy-elemental-isotope-analysis-learning-center/molecular-spectroscopy-information/ftir-information/ftir-sample-handling-techniques/ftir-sample-handling-tec. [Använd 3 06 2020].

[77] X. Chen, Z. Zhong, Z. Xu, L. Chen och Y. Wang, "2',7'-Dichlorodihydrofluorescein as a fluorescent probe for reactive oxygen species measurement: Forty years of application and controversy," *Free Radical Research ,* vol. 44, nr 10, pp. 587-604 , 2010.

[78] A. S. Keston och R. Brandt, ”The fluorometric analysis of ultramicro quantities of hydrogen peroxide,” *Analytical Biochemistry,* vol. 11, nr 1, pp. 1-5, 1965.

[79] E. Marchesi, C. Rota, Y. C. Fann, C. F. Chignell och R. P. Mason, ”Photoreduction of the fluorescent dye 2'-7'-dichlorofluorescein: a spin trapping and direct electron spin resonance study with implications for oxidative stress measurements,” *Free Radical Biology and Medicine,* vol. 26, nr 1-2, pp. 148-161, 1999.

[80] C. Rota, C. F. Chignell och R. P. Mason, ”Evidence for free radical formation during the oxidation of 2'-7'-dichlorofluorescin to the fluorescent dye 2'-7'-dichlorofluorescein by horseradish peroxidase:: Possible implications for oxidative stress measurements,” *Free Radical Biology and Medicine,* vol. 27, nr 7-8, pp. 873-881, 1999.

[81] T. M. Sager, D. W. Porter, V. A. Robinson, W. G. Lindsley, D. E. Schwegler-Berry och V. Castranova, ”Improved method to disperse nanoparticles for in vitro and in vivo investigation of toxicity,” *Nanotoxicology,* vol. 1, nr 2, pp. 118-129 , 2007.

[82] A. K. Pal, D. Bello, B. Budhlall, E. Rogers och D. K. Milton, ”Screening for Oxidative Stress Elicited by Engineered Nanomaterials: Evaluation of Acellular DCFH Assay,” *Sage,* vol. 10, nr 3, 2011.

[83] J. P. Gustafsson, ”Modeling the Acid–Base Properties and Metal Complexation of Humic Substances with the Stockholm Humic Model,” *Journal of Colloid and Interface Science ,* vol. 244, pp. 102-112, 2001.

[84] J. Ephraim, S. Alegret, A. Mathuthu, M. Bicking, R. L. Malcolm och J. A. Marinsky, ”A unified physicochemical description of the protonation and metal ion complexation equilibria of natural organic acids (humic and fulvic acids),” *Environmental Science & Technology,* vol. 20, nr 4, p. 354–366, 1986.

[85] E. Tipping och M. Hurley, ”A unifying model of cation binding by humic substances,” *Geochimica et Cosmochimica Acta,* vol. 56, nr 10, pp. 3627-3641, 1992.

[86] J. P. Gustafsson, *Visual MINTEQ 3.1 user guide,* Stockholm: Visual MINTEQ, 2014.

[87] S. Pradhan, J. Hedberg, E. Blomberg, S. Wold och I. Odnevall Wallinder, ”Effect of sonication on particle dispersion, administered dose and metal release of non-functionalized, non-inert metal nanoparticles.,” *Journal of Nanoparticle Research,* vol. 285, nr 18, 2016.

[88] perkinelmer, ”perkinelmer,” 2003. [Online]. Available: https://www.perkinelmer.com/Content/relatedmaterials/productnotes/prd_aanalyst700.pdf. [Använd 10 08 2020].

[89] Iowa state university, ”Iowa state university,” 19 12 2014. [Online]. Available: https://www.cif.iastate.edu/sites/default/files/uploads/Other_Inst/FTIR/Tensor%2037%20FTIR%20Operating%20Instructions.pdf. [Använd 10 09 2020].

[90] J. Gustafsson, ”Visual MINTEQ ver. 3.0. Based on de Allison JD, Brown DS, Novo-Gradac KJ, MINTEQA2 ver 4, 1991,” KTH Department of Land and Water Resources Engineering, Stockholm, 2011.

[91] S. J.Hug, "n SituFourier Transform Infrared Measurements of Sulfate Adsorption on Hematite in Aqueous Solutions," *Journal of Colloid and Interface Science,* vol. 188, nr 2, pp. 415-422, 1997.

[92] J. Degenhardt och A. J. McQuillan, "In Situ ATR-FTIR Spectroscopic Study of Adsorption of Perchlorate, Sulfate, and Thiosulfate Ions onto Chromium(III) Oxide Hydroxide Thin Films," *Langmuir,* vol. 13, nr 15, p. 4595–4602, 1999.

[93] H. Wijnja och C. P. Schulthess, "Vibrational Spectroscopy Study of Selenate and Sulfate Adsorption Mechanisms on Fe and Al (Hydr)oxide Surfaces," *Journal of Colloid and Interface Science,* vol. 299, nr 1, pp. 286-297, 2000.

[94] C. Su och D. L. Suarez, "In Situ Infrared Speciation of Adsorbed Carbonate on Aluminum and Iron Oxides," *Clays and Clay Mineral,* vol. 45, nr 6, pp. 814-82, 1997.

[95] H. Wijnja och C. Schulthess, "ATR–FTIR and DRIFT spectroscopy of carbonate species at the aged γ-Al2O3/water interface," *Spectrochimica Acta Part A: Molecular and Biomolecular Spectroscopy,* vol. 55, nr 4, pp. 861-872, 1999.

[96] M. B. Hay och S. C. Myneni, "Structural environments of carboxyl groups in natural organic molecules from terrestrial systems. Part 1: Infrared spectroscopy," *Geochimica et Cosmochimica Acta,* vol. 71, nr 14, pp. 3518-3532, 2007.

[97] S. Cabaniss, J. Leenheer och I. McVey, "Aqueous infrared carboxylate absorbances: aliphatic di-acids," *Spectrochim. Acta A,* vol. 54, pp. 449-458, 1998.

[98] S. Pradhan, J. Hedberg, J. Rosenqvist, C. M. Jonsson, S. Wold, E. Blomberg och I. Odnevall Wallinder, "Influence of humic acid and dihydroxy benzoic acid on the agglomeration, adsorption, sedimentation and dissolution of copper, manganese, aluminum and silica, nanoparticles – A tentative exposure scenario," *PLOS ONE,* 2018.

[99] G. Lefèvre, "In situ Fourier-transform infrared spectroscopy studies of inorganic ions adsorption on metal oxides and hydroxides," *Advances in Colloid and Interface Science,* vol. 107, nr 2-3, pp. 109-123, 2004.

[100] IUPAC, Compendium of Chemical Terminology, 2nd ed. (the "Gold Book"), Oxford: Blackwell Scientific Publications, 1997.

[101] T. M. C. Y. M. a. W. M. K. Tsao, "Origin, separation and identification of environmental nanoparticles: a review," *Journal of Environmental Monitoring,* vol. 13, pp. 1156-1163, 2011.

[102] P. MacCarthy, "The principles of humic substances," *Soil Science,* vol. 166, nr 11, p. 738–751, 2001.

[103] L. Grunberg, "The Formation of Hydrogen Peroxide on Fresh Metal Surfaces," *Proceedings of the Physical Society. Section B,* vol. 66, nr 3, p. 153, 1953.

[104] V. P. S. S. M. M. M. M. L. a. K. A. Aruoja, "Toxicity of 12 metal-based nanoparticles to algae, bacteria and protozoa," *Environmental Science: Nano,* nr 2, pp. 630-644, 2015.

[105] B. A. VanWinkle, K. L. De Mesy Bentley, J. M. Malecki, K. K. Gunter, I. M. Evans, A. Elder, J. N.

Finkelstein, G. Oberdörster och T. E. Gunter, ”Nanoparticle (NP) uptake by type I alveolar epithelial cells and their oxidant stress response,” *Nanotoxicology,* vol. 3, nr 4, pp. 307-318, 2009.

[106] K. Johnson, G. Purvis, Lopez-Capel, E., C. Peacock, N. Gray, T. Wagner, C. März, L. Bowen, J. Ojeda, N. Finlay, S. Robertson, F. Worrall och C. Greenwell, ”Towards a mechanistic understanding of carbon stabilization in manganese oxides,” *Nature Communications,* nr 6, p. 7628, 2015.

[107] W. Yao och F. J. Millero, ”Adsorption of Phosphate on Manganese Dioxide in Seawater,” *Environmental Science & Technology,* vol. 30, nr 2, p. 536–541, 1996.

TRITA ITM-EX 2020:607